Reactions of $[W_2(\eta\text{-}C_5H_4R)_2X_4]$ (R = Me or Pr^i, X = Cl or Br) with Lewis Bases and Synthesis of a Complex containing a Perpendicular Bridging Iminoacyl Ligand *

Qian Feng,[a] Montserrat Ferrer,[a] Malcolm L. H. Green,[a] Philip Mountford[a] and Victor S. B. Mtetwa[b]

[a] *Inorganic Chemistry Laboratory, South Parks Road, Oxford OX1 3QR, UK*

[b] *University of Swaziland, P/B 4, Kwaluseni, Manzini, Swaziland*

The W≡W triply bonded dimers $[W_2(\eta\text{-}C_5H_4R)_2X_4]$ (X = Cl, R = Pr^i **1a** or Me **1b**; X = Br, R = Pr^i **2**) readily undergo addition reactions with various Lewis bases to give the complexes $[W_2(\eta\text{-}C_5H_4Me)_2Cl_2(\mu\text{-}Cl)_2(dmpe)]$ [dmpe = 1,2-bis(dimethylphosphino)ethane],* $[W_2(\eta\text{-}C_5H_4R)_2Cl_2(\mu\text{-}Cl)_2(CO)_2]$,* *fac*-$[W(\eta\text{-}C_5H_4Pr^i)Br_3(CO)_2]$,* $[W_2(\eta\text{-}C_5H_4R)_2Cl_3(\mu\text{-}Cl)(\mu\text{-}\sigma{:}\eta^2\text{-}Bu^tNC)(Bu^tNC)]$, $[N(PPh_3)_2][W_2(\eta\text{-}C_5H_4R)_2Cl_4(\mu\text{-}Cl)]$ and $[W_2(\eta\text{-}C_5H_4R)_2Cl_3(\mu\text{-}Cl)(\mu\text{-}\sigma{:}\eta^2\text{-}R'CN)]$ (R' = Me, Et* or Ph; R = Pr^i or Me). Treatment of the last compounds with HCl affords the μ-iminoacyl derivatives *trans*- and *cis*-$[W_2(\eta\text{-}C_5H_4R)_2Cl_4(\mu\text{-}Cl)(\mu\text{-}R'CNH)]$.* The compounds labelled * have been crystallographically characterised.

The synthesis and reactivity of compounds containing metal–metal multiple bonds is of considerable interest.[1] A feature of many compounds in this class is their tendency to undergo ligand-addition reactions. Here we report some reactions of the W≡W triply bonded complexes $[W_2(\eta\text{-}C_5H_4R)_2X_4]$ (X = Cl, R = Pr^i **1a** or Me **1b**; X = Br, R = Pr^i **2**)[2] with Lewis bases. Part of this work has been communicated.[3]

Results and Discussion

Reaction with dmpe [1,2-*bis*(*dimethylphosphino*)*ethane*].—Treatment of a toluene solution of $[W_2(\eta\text{-}C_5H_4Me)_2Cl_4]$ **1b** with dmpe for 12 h caused a colour change from emerald green to red and red crystals of $[W_2(\eta\text{-}C_5H_4Me)_2Cl_2(\mu\text{-}Cl)_2(dmpe)]$ **3** could be isolated in *ca.* 25% yield (Scheme 1). Compound **3** was characterised by elemental analysis, ^{1}H and ^{31}P-{^{1}H} NMR spectroscopy, and by a single crystal X-ray diffraction analysis. Characteristing data for **3**, and all the other new compounds described herein, are given in Table 1 and will not be discussed further except where their interpretation is not straightforward. The molecular structure of **3** is shown in Fig. 1. Details of the crystal structure determination have been described elsewhere.[4]

The solid-state structure of complex **3** consists of a $W(\eta\text{-}C_5H_4Me)Cl_2$ unit and a $W(\eta\text{-}C_5H_4Me)(dmpe)$ unit linked by two μ-chloro bridges. The $W(\mu\text{-}Cl)_2W$ core is non-planar with a hinge angle [Cl(1)–W(1)–Cl(2) plane] to [Cl(1)–W(2)–Cl(2) plane] of 116.4°. The two tungsten atoms are separated by a distance of 3.196(1) Å, suggestive of a significant degree of metal–metal bonding. It is possible to assign a W^{III}_2 representation to **3** whereby the structure can be considered to consist of two otherwise 17-electron fragments joined by a metal–metal single bond. Although the metal–metal separation is relatively long for a tungsten–tungsten single bond, it is noteworthy that the unsupported metal–metal single bond in $[W_2(\eta\text{-}C_5H_5)_2(CO)_6]$ has a length of 3.222(1) Å.[5] The geometry of the $W(\eta\text{-}C_5H_4Me)Cl_4$ fragment in **3** is very similar to that found for monomeric $[W(\eta\text{-}C_5H_4Pr^i)Cl_4]$,[2] and that of the $W(\eta\text{-}C_5H_4Me)(dmpe)(\mu\text{-}Cl)_2$ fragment is analogous to that found for $[Mo(\eta\text{-}C_5H_4Pr^i)Cl_2(dmpe)]$.[6]

A puckered metallacore geometry appears to be a common feature of dinuclear species containing a *cis*-$M_2(\eta\text{-}C_2H_5)_2(\mu\text{-}L)_2$ fragment. For example, the compounds $[Mo_2(\eta\text{-}C_5H_5)_2O_2(\mu\text{-}O)_2]$,[7] $[Re_2(\eta\text{-}C_5Me_4Et)_2Cl_4(\mu\text{-}Cl)_2]$,[8] $[Nb_2(\eta\text{-}C_5H_4Me)_2(CO)_4(\mu\text{-}Cl)_2]$[9] and $[Fe_2(\eta\text{-}C_5H_5)_2(CO)_2(\mu\text{-}CO)_2]$[10] all possess a *cis* disposition of the $\eta\text{-}C_5R_5$ rings and a non-planar $M_2(\mu\text{-}L)_2$ core. The puckered $M_2(\mu\text{-}L)_2$ cores in $[Mo_2(\eta\text{-}C_5H_5)_2O_2(\mu\text{-}O)_2]$ and $[Fe_2(\eta\text{-}C_5H_5)_2(CO)_2(\mu\text{-}CO)_2]$ have been rationalised using molecular orbital calculations[11] which suggest that folding the bridging ligands away from or towards the $\eta\text{-}C_5R_5$ moieties maximises metal–μ-ligand π overlaps, and that the direction of folding depends on the π-donor/π-acceptor characteristics of the bridging ligands.

The solution ^{1}H and ^{31}P NMR spectra of complex **3** are consistent with the solid-state structure. Thus the ^{1}H spectrum shows resonances assignable to a co-ordinated dmpe ligand and to two $\eta\text{-}C_5H_4Me$ moieties, only one of which shows coupling to the ^{31}P nuclei of the dmpe ligand.

In contrast to the behaviour of **1b**, treatment of the related quadruply bridged dimolybdenum complex $[Mo_2(\eta\text{-}C_5H_4Pr^i)_2(\mu\text{-}Cl)_4]$ with dmpe or monodentate phosphines leads to cleavage of the dimolybdenum dimer and compounds analogous to **3** are not observed.[12]

Reaction with Carbon Monoxide.—Treatment of toluene solutions of complex **1** with carbon monoxide (1 atm) gave orange-brown microcrystals of $[W_2(\eta\text{-}C_5H_4R)_2Cl_2(\mu\text{-}Cl)_2(CO)_2]$ (R = Pr^i **4a** or Me **4b**) in near-quantitative yield. The compounds were characterised by elemental analysis, IR and ^{1}H and ^{13}C NMR spectroscopy. For **4b** a single-crystal X-ray diffraction analysis was carried out. The molecular structure is shown in Fig. 2, selected bond lengths and angles are given in Table 2, and fractional atomic coordinates for the non-hydrogen atoms are listed in Table 3.

The molecular structure of complex **4b** is closely similar to that of **3**. Notably, however, the CO ligands of **4b** favour a 1,2 mode of co-ordination to the ditungsten centre in contrast to the 1,1 mode necessarily adopted by the chelating dmpe ligand of **3**. The W(1)–W(1B) bond length [2.9647(8) Å] is somewhat shorter than that of **3** and the hinge angle of the puckered $W(\mu\text{-}Cl)_2W$ core {[Cl(1)–W(1)–Cl(1B) plane] to [Cl(1)–W(1B)–

---

* *Supplementary data available:* see Instructions for Authors, *J. Chem. Soc., Dalton Trans.*, 1992, Issue 1, pp. xx–xxv.

Non-SI units employed: atm = 101 325 Pa, cal = 4.184 J.

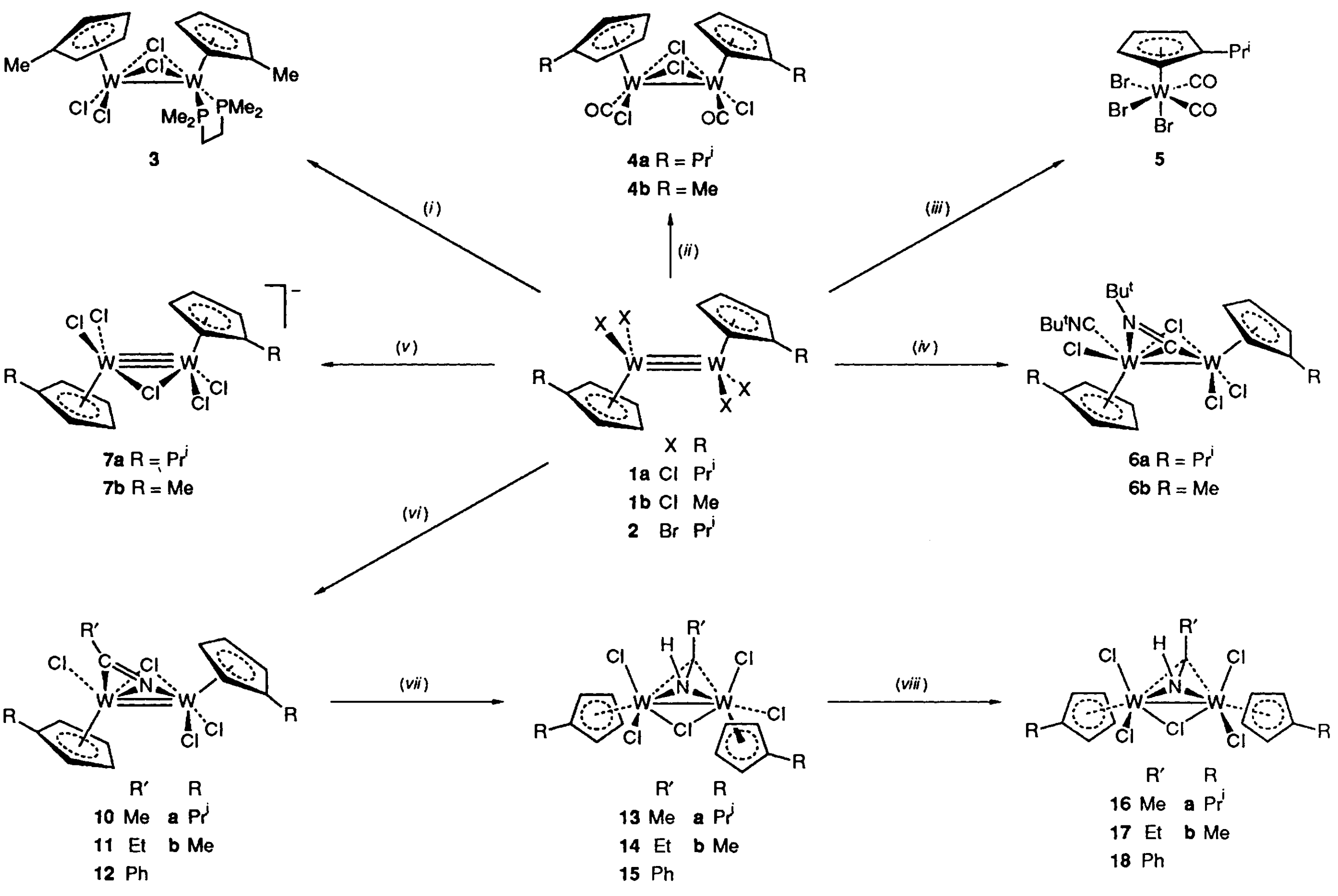

Scheme 1 *Reagents and conditions:* (*i*) dmpe, toluene, 12 h, yield 25%; (*ii*) CO (1 atm) toluene, 12 h, 90%; (*iii*) CO (1 atm), toluene, 12 h, 40%; (*iv*) Bu^{t}NC, diethyl ether, 12 h, 75–80%; (*v*) [N(PPh$_3$)$_2$]Cl, dichloromethane, 1 h, 80–95%; (*vi*) R′CN, light petroleum (b.p. 40–60 °C), 30 min, 70–90%; (*vii*) HCl (g), diethyl ether, 3 min, 85–90%; (*viii*) dichloromethane, 30 min, >95%. All reactions at r.t.

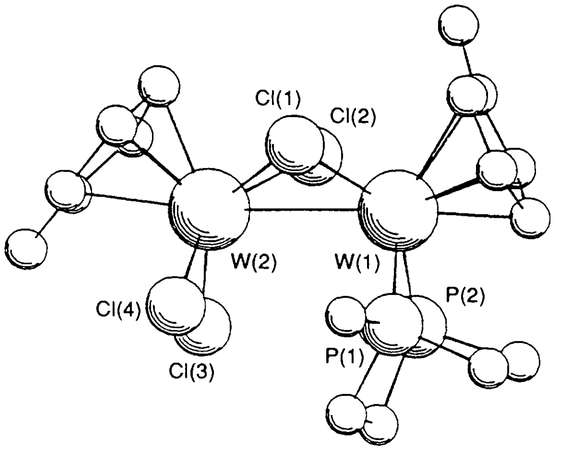

Fig. 1 Molecular structure of [W$_2$(η-C$_5$H$_4$Me)$_2$Cl$_2$(μ-Cl)$_2$(dmpe)] **3**. Hydrogen atoms are omitted for clarity

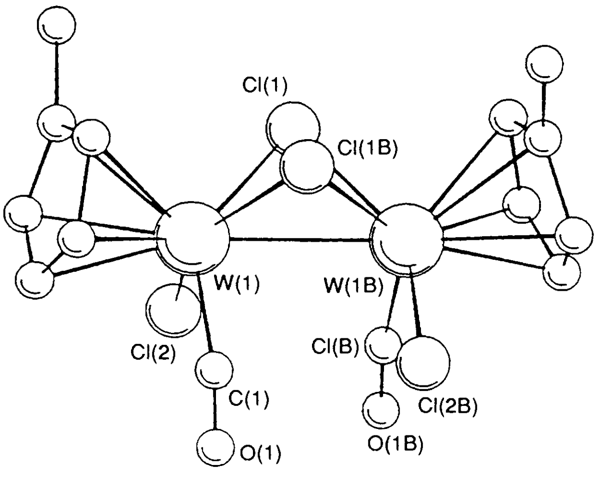

Fig. 2 Molecular structure of [W$_2$(η-C$_5$H$_4$Me)$_2$Cl$_2$(μ-Cl)$_2$(CO)$_2$] **4b**. Hydrogen atoms are omitted for clarity. The molecule lies across a crystallographic two-fold rotation axis; atoms labelled 'B' are related to their counterparts by the symmetry operator −*x*, *y*, −*z*

Cl(1B) plane] of 97.7°} is correspondingly more acute. These observations may reflect the very different σ-donor and π-acceptor characteristics of the CO and dmpe ligands.

The solid-state (KBr) and solution (CH$_2$Cl$_2$) IR spectra of complexes **4a** and **4b** show strong bands at *ca.* 1986 and 1954, and 1970 and 1935 cm^{-1} respectively assignable to ν(C≡O). The ^{1}H and ^{13}C NMR spectra of freshly prepared solutions are consistent with the solid-state structure shown in Fig. 2. They show resonances assignable to one type of diastereotopic η-C$_5$H$_4$R moiety, and the ^{13}C spectra have an additional singlet at δ *ca.* 225 [^1J(^{13}C–^{183}W) = 188 Hz, *ca.* 14% of total satellite intensity, for **4a*** (prepared from **1a** and ^{13}C-enriched carbon monoxide)].

Compound **4a** isomerises slowly in dichloromethane solution to give an equilibrium mixture of **4a** and a new compound in a *ca.* 1 : 1 molar ratio (assuming the new species to be dinuclear). Thus the ^{1}H and ^{13}C-{^{1}H} NMR spectra of solutions of **4a** which have been allowed to stand for 4–5 h at room temperature (r.t.) show an additional set of resonances assignable to *two* types of diastereotopic η-C$_5$H$_4$R ligands; the ^{13}C spectra show an additional two singlets assignable to CO at δ 220.1 and 235.4 [^1J(^{13}C–^{183}W) = 195 and 156 Hz respectively, the satellite pairs each having *ca.* 14% of total signal intensity, for the isomer of **4a***]. The ^{1}H NMR data show that the total signal intensity does not change during the equilibration process and an elemental analysis of the isomeric mixture obtained from a dichloromethane solution of **4a** was identical (within error) to that obtained for the first-formed pure compound. Solutions of the methylcyclopentadienyl complex **4b** show similar behaviour.

The solution IR spectrum of the equilibrium mixture of complex **4a** in dichloromethane shows an additional band of

Table 1 Analytical and spectroscopic data

Compound	Colour	Analysis[a] (%) C	H	N	Halide	NMR[b]
3	Red	26.6 (26.4)	3.8 (3.7)		16.9 (17.3)	^{1}H: 5.01, 4.56 [2 × virtual t, 2 × 2 H, WCl$_2$(η-C$_5$*H*$_4$Me)], 4.14, 4.06 [2 × t of virtual t, 2 × 2 H, *J*(^{1}H–^{31}P) 0.5, W(η-C$_5$*H*$_4$Me)(dpme)], 3.79 (m, 2 H, C*H*$_2$PMe$_2$), 2.02 ['filled-in' d, 6 H, *J*(^{1}H–^{31}P), 7.4, P*Me*$_\mathrm{A}$Me$_\mathrm{B}$ or PMe$_\mathrm{A}$*Me*$_\mathrm{B}$], 1.94, 1.89 (2 × s, 2 × 3 H, η-C$_5$H$_4$*Me*), 0.89 (m, 2 H, C*H*$_2$PMe$_2$), 0.35 ['filled-in' d, 6 H, *J*(^{1}H–^{31}P) 7.4, P*Me*$_\mathrm{B}$Me$_\mathrm{A}$ or PMe$_\mathrm{B}$*Me*$_\mathrm{A}$] ^{31}P-{^{1}H}: −28.2
4a[c]	Orange-brown	27.6 (27.7)	2.7 (2.8)		18.0 (18.2)	^{1}H:[d] 5.74, 5.65, 5.27, 5.18 (4 × virtual q, 4 × 2 H, η-C$_5$*H*$_4$Pr$^\mathrm{i}$), 2.75 (spt, 2 H, *J* 6.9, C*H*Me$_2$), 1.28 (overlapping 2 × d, 12 H, *J* 6.9, CH*Me*$_2$) ^{13}C-{^{1}H}:[d] 223.4, [^{1}*J*(^{13}C–^{183}W) 187.6, CO], 130.3 (*C*Pr$^\mathrm{i}$), 104.3, 92.4, 86.9, 84.5 (4 × CH of η-*C*$_5$H$_4$Pr$^\mathrm{i}$), 28.1 (*C*HMe$_2$), 22.5, 21.4 (2 × CH*Me*$_2$)
4b[c]	Orange-brown	23.3 (23.2)	2.0 (1.95)		19.2 (19.6)	^{1}H:[d] 5.67, 5.55, 5.33, 5.20 (4 × virtual q, 4 × 2 H, η-C$_5$*H*$_4$Me), 2.26 (s, 6 H, Me)
5[f]	Yellow	20.6 (20.5)	1.8 (1.9)		39.9 (40.3)	^{1}H:[d] 5.72, 5.67 (2 × virtual t, 2 × 2 H, η-C$_5$*H*$_4$Pr$^\mathrm{i}$), 3.20 (spt, 1 H, *J* 6.9, C*H*Me$_2$), 1.34 (d, 6 H, *J* 6.9, CH*Me*$_2$) ^{13}C-{^{1}H}:[d] 187.9 (CO), 136.0 (*C*Pr$^\mathrm{i}$), 97.1, 85.9 (2 × CH of η-*C*$_5$H$_4$Pr$^\mathrm{i}$), 30.5 (*C*HMe$_2$), 22.6 (CH*Me*$_2$)
6a[g]	Red-purple	35.5 (35.1)	4.5 (4.5)	3.1 (3.1)	22.3 (22.0)	^{1}H: 6.30, 5.41, 5.34, 5.19, 5.07, 5.02, 4.60, 4.20 (8 × virtual q, 8 × 1 H, η-C$_5$*H*$_4$Pr$^\mathrm{i}$), 3.06 (overlapping 2 × spt, 2 H, *J* 6.9, C*H*Me$_2$), 1.46 (s, 9 H, μ-Bu$^\mathrm{t}$NC), 1.33 (d, 3 H, *J* 6.9, CH*Me*$_2$), 1.23 (s, 9 H, Bu$^\mathrm{t}$NC), 1.18, 1.15, 1.03 (3 × d, 3 × 3 H, *J* 6.9, CH*Me*$_2$) ^{13}C: 232.2(μ-σ:η^2-Bu$^\mathrm{t}$N*C*), 146.0 (Bu$^\mathrm{t}$N*C*), 134.6, 134.0 (2 × *C*Pr$^\mathrm{i}$), 106.3, 98.2, 95.9, 92.0, 91.7, 90.8, 86.3, 86.0 (8 × CH of η-*C*$_5$H$_4$Pr$^\mathrm{i}$), 63.7 [μ-σ:η^2-*C*(CH$_3$)$_3$NC], 57.5 [*C*(CH$_3$)$_3$NC], 32.6 [s, μ-σ:η^2-C(*C*H$_3$)$_3$NC], 30.0 [C(*C*H$_3$)$_3$NC], 28.9, 28.4 (2 × *C*HMe$_2$), 23.1, 22.7, 21.6, 21.4 (4 × CH*Me*$_2$)
6b[h]	Red-purple	31.7 (31.7)	3.8 (3.8)	3.3 (3.4)	17.2 (17.2)	^{1}H: 6.13, 5.24, 5.13, 5.10, 5.08, 4.83, 4.42, 4.37 (8 × virtual q, 8 × 1 H, η-C$_5$*H*$_4$Me), 2.08, 2.01 (2 × s, 2 × 3 H, η-C$_5$H$_4$*Me*), 1.42 (s, 9 H, μ-Bu$^\mathrm{t}$NC), 1.21 (s, 9 H, Bu$^\mathrm{t}$NC) ^{13}C: 231.1 [μ-σ:η^2-Bu$^\mathrm{t}$N*C*, ^{1}*J*(^{13}C–^{183}W) 155.8, *ca.* 28% of total signal intensity), 146.5 (Bu$^\mathrm{t}$N*C*), 123.4, 122.8 (2 × *C*Me of η-*C*$_5$H$_4$Me) 105.9, 100.0, 98.3, 96.9, 93.1, 91.1, 87.6, 87.5 (8 × CH of η-*C*$_5$H$_4$Me), 63.5 [μ-σ:η^2-*C*(CH$_3$)$_3$NC], 57.5 [*C*(CH$_3$)$_3$NC], 32.6 [s, μ-σ:η^2-C(*C*H$_3$)$_3$NC], 30.2 [C(*C*H$_3$)$_3$NC], 16.0, 15.3 (2 × η-C$_5$H$_4$*Me*)
7a	Green	48.1 (48.1)	4.0 (4.0)	1.1 (1.1)	13.8 (13.7)	^{1}H:[d,i] 7.66–7.48 [m, 30 H, N(PPh$_3$)$_2$], 6.82, 6.60, 5.14, 4.93 (4 × br m, 4 × 2 H, η-C$_5$*H*$_4$Pr$^\mathrm{i}$), 2.13 (spt, 2 H, *J* 6.9, C*H*Me$_2$), 0.95, 0.86 (2 × d, 2 × 6 H, *J* 6.9, CH*Me*$_2$) ^{13}C-{^{1}H}:[d,i] 134.1, 132.3 [2 × N(PPh$_3$)$_2$], 130.5 (*C*Pr$^\mathrm{i}$), 130.0 [N(PPh$_3$)$_2$], 127.0 [d, ^{1}*J*(^{13}C–^{31}P) 107.2, *ipso*-C of N(PPh$_3$)$_2$], 105.6, 99.9, 97.7, 96.0 (4 × CH of η-*C*$_5$H$_4$Pr$^\mathrm{i}$), 27.1 (*C*HMe$_2$), 22.7, 21.7 (2 × CH*Me*$_2$)
7b	Green[j]	47.1 (47.5)	3.8 (4.0)	1.1 (1.1)	14.7 (13.4)	^{1}H:[d,i] 7.65–7.47 [m, 30 H, N(PPh$_3$)$_2$], 6.75 (overlapping 2 × br m, 4 H, η-C$_5$*H*$_4$Me), 4.98, 4.93 (2 × br m, 2 × 2 H, η-C$_5$*H*$_4$Me), 3.67 (br m, 4 H, OC*H*$_2$CH$_2$), 1.78 (br m, 4 H, OCH$_2$C*H*$_2$), 1.63 (s, 6 H, Me)
8	Brown	55.1 (55.1)	4.2 (4.2)	1.4 (1.3)	16.2 (16.5)	^{1}H:[d,i] 7.45–7.20 [m, 30 H, N(PPh$_3$)$_2$], 6.78, 6.72, 5.12, 4.93 (4 × br m, 4 × 2 H, η-C$_5$*H*$_4$Me), 1.37 (s, 6 H, η-C$_5$H$_4$*Me*) ^{13}C-{^{1}H}:[d,i] 132.2 (*C*Me), 129.0, 126.4, 124.6 [N(PPh$_3$)$_2$], 122.6 [d, *J* 113, *ipso*-C of N(PPh$_3$)$_2$], 106.5, 100.0, 99.0, 96.3 (4 × CH of η-*C*$_5$H$_4$Me), 8.0 (Me)
10a	Brown	28.5 (28.3)	3.4 (3.3)	1.8 (1.8)	18.1 (18.5)	^{1}H: 6.33, 5.60 (2 × virtual q, 2 × 1 H, η-C$_5$*H*$_4$Pr$^\mathrm{i}$), 5.42 (overlapping 2 × virtual q, 2 H, η-C$_5$*H*$_4$Pr$^\mathrm{i}$), 5.33, 5.28, 5.20, 4.99 (4 × virtual q, 4 × 1 H, C$_5$*H*$_4$Pr$^\mathrm{i}$), 3.42 (s, 3 H, μ-σ:η^2-MeCN), 3.22, 2.91 (2 × spt, 2 × 1 H, *J* 6.9, C*H*Me$_2$), 1.30–1.0 (4 × d, 4 × 3 H, *J* 6.9, CH*Me*$_2$) ^{13}C-{^{1}H}: 240.7 [^{1}*J*(^{13}C–^{183}W) 98 (*ca.* 14.1% by area), μ-σ:η^2-Me*C*N), 130.8, 130.4 (2 × *C*Pr$^\mathrm{i}$), 105.4, 105.0, 103.4, 101.8, 100.8, 97.8, 90.7 (8 × CH of η-*C*$_5$H$_4$Pr$^\mathrm{i}$, two signals overlapping), 29.2, 28.8 (2 × *C*HMe$_2$), 26.3 (μ-σ:η^2-*Me*CN), 23.8, 23.0, 22.7, 22.4 (4 × CH*Me*$_2$)
10b	Brown	23.3 (23.7)	2.35 (2.4)	1.6 (2.0)	19.5 (20.0)	^{1}H: 5.88, 5.65, 5.40 (3 × virtual q, 3 × 1 H, η-C$_5$*H*$_4$Me), 5.35 (overlapping 2 × virtual q, 2 H, η-C$_5$*H*$_4$Me), 5.20, 5.05, 4.67 (3 × virtual q, 3 × 1 H, η-C$_5$*H*$_4$Me), 3.35 (s, 3 H, μ-σ:η^2-MeCN), 2.15, 2.07 (2 × s, 2 × 3 H, η-C$_5$H$_4$*Me*)

Table 1 (*continued*)

Compound	Colour	Analysis[a] (%)				NMR[b]
		C	H	N	Halide	
11a[k]	Brown					^{1}H: 6.31, 5.80, 5.48, 5.40 (4 × virtual q, 4 × 1 H, η-C$_5H_4$Pr^i), 5.37 (overlapping 2 × virtual q, 2 H, η-C$_5H_4$Pr^i), 5.24, 5.01 (2 × virtual q, 2 × 1 H, η-C$_5H_4$Pr^i), 3.82 (overlapping 2 × d of q, 2 × 1 H, ^2J 13.5, ^3J 7.4, μ-σ : η^2-MeCH_2CN), 3.30, 2.90 (2 × spt, 1 H, J 6.9, CHMe$_2$), 1.18 (d, 3 H, J 6.9, CHMe_2), 1.17 (t, 3 H, J 7.4, μ-σ:η^2-MeCH$_2$CN), 1.16, 1.11, 1.07 (3 × d, 3 × 3 H, J 6.9, CHMe_2) ^{13}C-{^{1}H}: 245.7 [^1J(^{13}C–^{183}W) 98 (*ca.* 14% by area), μ-σ:η^2-MeCH$_2C$N], 132.9, 131.8 (2 × CPr^i), 103.9, 103.5, 98.3, 98.0, 97.8, 89.3 (8 × CH of η-C_5H$_4$Pr^i, 2 × 2 signals overlapping), 34.5 (μ-σ:η^2-MeCH$_2$CN), 29.3, 28.7 (2 × CHMe$_2$), 24.0, 22.7, 22.5, 22.2 (4 × CHMe_2), 13.2 (μ-σ:η^2-MeCH$_2$CN)
11b	Brown	24.4 (24.9)	2.6 (2.65)	1.6 (1.9)	20.05 (19.6)	^{1}H: 5.90, 5.65, 5.51 (3 × virtual q, 3 × 1 H, η-C$_5H_4$Me), 5.37 (overlapping 2 × virtual q, 2 H, η-C$_5H_4$Me), 5.18, 5.14, 4.64 (3 × virtual q, 3 × 1 H, η-C$_5H_4$Me), 3.69 (overlapping 2 × d of q, ^2J 14.2, ^3J 7.4, μ-σ:η^2-MeCH_2CN), 2.18, 2.05 (2 × s, 2 × 3 H, η-C$_5$H$_4$$Me$), 1.11 (t, 3 H, J 7.4, μ-σ:η^2-MeCH$_2$CN)
12a	Brown	32.1 (32.3)	3.3 (3.3)	1.5 (1.6)	16.8 (17.1)	^{1}H: 7.89 (d 2, H, J 7.0, *o*-H of Ph), 7.35, (t, 2 H, J 7.6, *m*-H of Ph), 6.95 (t, 1 H, J 7.6, *p*-H of Ph), 6.45, 5.96, 5.60, 5.52 (4 × virtual q, 4 × 1 H, η-C$_5H_4$Pr^i), 5.27 (overlapping 2 × virtual q, 2 H, η-C$_5H_4$Pr^i), 5.13, 4.93 (2 × virtual q, 2 × 1 H, η-C$_5H_4$Pr^i), 2.92 (2 × spt, 2 × 1 H, J 6.9, CHMe$_2$), 1.19, 1.14, 1.10, 1.03 (4 × d, 4 × 3 H, J 6.9, CHMe_2) ^{13}C-{^{1}H}: 234.6 [^1J(^{13}C–^{183}W) 93 (*ca.* 14% by area), μ-σ:η-PhCN), 135.2, 134.7 (2 × CPr^i), 132.7, 132.6, 131.9 (*ipso*-, *o*-, *m*- and *p*-C of Ph, two signals overlapping or obscured by solvent), 106.6, 104.8, 103.4, 102.1, 99.4, 99.1, 97.2, 88.9 (8 × CH of η-C_5H$_4$Pr^i), 29.2, 28.5 (2 × CHMe$_2$), 24.1, 22.6, 21.9 (4 × CHMe_2, two signals overlapping)
12b	Brown	29.5 (29.6)	2.4 (2.8)	1.7 (1.8)	18.5 (18.4)	^{1}H: 7.82 (d, 2 H, J 7.2, *o*-H of Ph), 7.32 (t, 2 H, J 7.4, *m*-H of Ph), 6.94 (t, 1 H, J 7.4, *p*-H of Ph), 5.98, 5.67, 5.60, 5.46 (4 × virtual q, 4 × 1 H, η-C$_5H_4$Me), 5.30 (overlapping 2 × virtual q, 2 H, η-C$_5H_4$Me), 5.12, 4.61 (2 × virtual q, 2 × 1 H, η-C$_5H_4$Me), 2.19, 1.98 (2 × s, 2 × 3 H, Me)
13a	Orange	27.2 (27.0)	3.3 (3.3)	1.7 (1.75)	22.3 (22.0)	^{1}H:[l] 11.20 (br s, 1 H, μ-MeCNH), 6.44 (virtual q, 1 H, η-C$_5H_4$Pr^i), 6.20 (overlapping 2 × virtual q, 2 H, η-C$_5H_4$Pr^i), 6.12, 6.07, 5.77, 5.65 5.33 (5 × virtual q, 5 × 1 H, η-C$_5H_4$Pr^i), 3.65 (s, 3 H, μ-MeCNH), 3.09, 2.91 (2 × spt, 2 × 1 H, J 6.9, CHMe$_2$), 1.28 (d 3, H, J 6.9, CHMe_2), 1.25 (overlapping 2 × d, 6 H, J 6.9, CHMe_2), 1.18 (d, 3 H, J 6.9, CHMe_2) ^{13}C-{^{1}H}:[l] 141.7 (μ-MeCNH), 137.5, 132.7 (2 × CPr^i), 113.2, 112.6, 106.7, 104.5, 98.7, 98.2, 95.7. 94.7 (8 × CH of η-C_5H$_4$Pr^i), 28.3, 27.5 (2 × CHMe$_2$), 27.1 (μ-MeCNH), 22.5, 22.2, 21.5, 21.3 (CHMe_2)
13b	Orange	22.3 (22.6)	2.4 (2.4)	1.7 (1.9)	23.1 (23.8)	^{1}H:[l,m] 11.17 (br s, 1 H, μ-MeCNH), 6.31 (virtual q, 1 H, η-C$_5H_4$Me), 6.16 (overlapping 2 × virtual q, 2 H, η-C$_5H_4$Me), 6.03, 5.94, 5.67, 5.61, 5.35 (5 × virtual q, 5 × 1 H, η-C$_5H_4$Me), 3.56 (s, 3 H, μ-MeCNH), 2.34, 2.24 (2 × s, 2 × 3 H, η-C$_5$H$_4$$Me$)
14a[n]	Orange	28.2 (27.9)	3.5 (3.4)	1.7 (1.7)	21.5 (21.7)	^{1}H:[l] 11.35 (br s, 1 H, μ-EtCNH), 6.42, 6.24, 6.20, 6.15, 6.09, 5.73, 5.70, 5.30 (8 × virtual q, 8 × 1 H, η-C$_5H_4$Pr^i), 4.41 (overlapping 2 × d of q, 2 H, ^2J 9.2, ^3J 8.0, μ-MeCH_2CNH), 3.07, 2.90 (2 × spt, 2 × 1 H, J 6.9, CHMe$_2$), 1.27–1.14 (overlapping 4 × d + t, 15 H, CHMe_2 + μ-MeCH$_2$CNH) ^{13}C-{^{1}H}:[l] 141.6 (μ-MeCH$_2C$NH), 137.1, 132.9 (2 × CPr^i), 133.5, 112.7, 105.9, 104.2, 98.9, 97.3, 96.2, 94.5 (8 × CH of η-C_5H$_4$Pr^i), 30.8 (μ-MeCH$_2$CNH), 28.2, 27.4 (2 × CHMe$_2$), 22.3, 22.1, 21.6, 21.5 (4 × CHMe_2), 15.4 (μ-MeCH$_2$CNH)
14b	Orange	23.3 (23.7)	2.6 (2.7)	1.8 (1.8)	23.1 (23.35)	^{1}H:[l,m] 11.40 (br s, 1 H, μ-EtCNH), 6.38 (virtual q, 1 H, η-C$_5H_4$Me), 6.21 (overlapping 2 × virtual q, 2 × 1 H, η-C$_5H_4$Me), 6.10, 6.01, 5.75, 5.68, 5.37 (5 × virtual q, 5 × 1 H, η-C$_5H_4$Me), 4.42, 4.28 (2 × d of q, 2 × 1 H, ^2J 9.5, ^3J 8.0, μ-MeCH_2CNH), 2.37, 2.25 (2 × s, 2 × 3 H, η-C$_5H_4$Me), 2.05 (t 3, H, J 8.0, μ-MeCH$_2$CNH)
15a	Orange	31.8 (32.0)	3.3 (3.3)	1.6 (1.6)	20.3 (20.5)	^{1}H:[l] 11.96 (br s, 1 H, μ-PhCNH), 7.39 (m, 3 H, C$_6H_5$CNH), 7.35 (m, 2 H, C$_6H_5$CNH), 6.49 (overlapping 2 × virtual q, 2 H, η-C$_5H_4$Pr^i), 6.30 (virtual q, 1 H, η-C$_5H_4$Pr^i), 5.89 (overlapping 2 × virtual q, 2 H, η-C$_5H_4$Pr^i), 5.75, 5.58, 5.42 (3 × virtual q, 3 × 1 H, η-C$_5H_4$Pr^i), 2.93, 2.82 (2 × spt, 2 × 1 H, J 6.9, CHMe$_2$), 1.20, 1.17, 1.14, 0.79 (4 × d, 4 × 3 H, J 6.9, CHMe_2) ^{13}C-{^{1}H}:[l] 142.4 (μ-PhCNH), 140.5 (C_6H$_5$CNH), 134.8, 132.4 (2 × CPr^i), 128.9, 128.1, 126.2 (3 × C_6H$_5$CNH), 112.2, 110.7, 108.5, 105.3, 100.3, 100.0, 97.4, 94.8 (8 × CH of η-C_5H$_4$Pr^i), 28.2, 27.6 (2 × CHMe$_2$), 22.4, 21.9, 21.8, 20.0 (4 × CHMe_2)
15b	Orange	28.2 (28.3)	2.45 (2.5)	1.6 (1.7)	22.2 (22.0)	^{1}H:[l,m] 12.0 (br s, 1 H, μ-PhCNH), 7.43 (m, 3 H, C$_6H_5$CNH), 7.11 (m, 2 H, C$_6H_5$CNH), 6.45 (overlapping 2 × virtual q, 2 H, η-C$_5H_4$Me), 6.19, 5.97, 5.82 (3 × virtual q, 3 × 1 H, η-C$_5H_4$Me), 5.68 (overlapping 2 × virtual q, 2 H, η-C$_5H_4$Me), 5.49 (virtual q, 1 H, η-C$_5H_4$Me), 2.28, 2.18 (2 × s, 2 × 3 H, Me)

Table 1 (*continued*)

		Analysis[a] (%)				
Compound	Colour	C	H	N	Halide	NMR[b]
16a[o]	Purple	27.1 (27.0)	3.3 (3.3)	1.7 (1.75)	21.7 (22.0)	^{1}H:[d] 6.20 (br m, 2 H, η-C$_5$*H*$_4$Pr^i), 5.89 (br s, 1 H, μ-MeCN*H*), 5.73, 5.17, 4.78 (3 × br m, 3 × 2 H, η-C$_5$*H*$_4$Pr^i), 3.91 (s, 3 H, μ-*Me*CNH), 3.52 (spt, 2 H, *J* 6.9, C*H*Me$_2$), 1.45, 1.38 (2 × d, 2 × 6 H, *J* 6.9, CH*Me*$_2$) ^{13}C-{^{1}H}:[d] 141.0 [$^1J(^{13}C-^{183}W)$ 34 (*ca.* 26% by area), μ-Me*C*NH], 134.8 (*C*Pr^i), 114.6, 105.7, 100.4, 98.8 (4 × CH of η-*C*$_5$H$_4$Pr^i), 28.1 (*C*HMe$_2$), 27.2 (μ-*Me*CNH), 22.5, 21.5 (2 × CH*Me*$_2$)
16b	Purple	22.6 (22.6)	2.4 (2.4)	1.8 (1.9)	20.55 (23.8)	^{1}H: [l,m] 9.54 (br s, 1 H, μ-MeCN*H*), 5.99, 5.95, 5.50, 5.47 (4 × br m, 4 × 2 H, η-C$_5$*H*$_4$Me), 3.71 (s, 3 H, μ-*Me*CNH), 2.53 (s, 6 H, η-C$_5$H$_4$*Me*)
17a[o]	Purple	27.6 (27.9)	3.4 (3.4)	1.7 (1.7)	21.5 (21.7)	^{1}H:[d] 6.20, 6.03 (2 × virtual q, 2 × 2 H, η-C$_5$*H*$_4$Pr^i), 5.89 (br s, 1 H, μ-EtCN*H*), 5.19, 4.87 (2 × virtual q, 2 × 2 H, η-C$_5$*H*$_4$Pr^i), 4.62 (q, 2 H, *J* 7.5, μ-MeC*H*$_2$CNH), 3.51 (spt, 2 H, *J* 6.9, C*H*Me$_2$), 1.42, 1.37 (2 × d, 2 × 6 H, *J* 6.9, CH*Me*$_2$), 1.36 (t, 3 H, *J* 7.5, μ-*Me*CH$_2$CNH) ^{13}C-{^{1}H}:[d] 141.9 [$^1J(^{13}C-^{183}W)$ 34 (*ca.* 26% by area), μ-Et*C*NH], 135.2 (*C*Pr^i), 114.3, 104.8, 97.6, 96.4 (4 × CH of η-*C*$_5$H$_4$Pr^i), 33.7 (μ-Me*C*H$_2$CNH), 27.8 (*C*HMe$_2$), 22.8, 21.4 (2 × CH*Me*$_2$), 14.1 (μ-*Me*CH$_2$CNH)
17b[o]	Purple	23.7 (23.7)	2.6 (2.7)	1.75 (1.8)	22.9 (23.35)	^{1}H:[d] 6.07, 5.95 (2 × virtual q, 2 × 2 H, η-C$_5$*H*$_4$Me), 5.89 (br s, 1 H, μ-EtCN*H*), 5.15, 5.02 (2 × virtual q, 2 × 2 H, η-C$_5$*H*$_4$Me), 4.61 (q, 2 H, *J* 7.5, μ-MeC*H*$_2$CNH), 2.69 (s, 6 H, η-C$_5$H$_4$*Me*), 1.32 (t, 3 H, *J* 7.5, μ-*Me*CH$_2$CNH)
18a[p]	Purple	31.8 (32.0)	3.3 (3.3)	1.6 (1.6)	20.3 (20.5)	^{1}H:[l] 10.40 (br s, 1 H, μ-PhCN*H*), 7.30 (overlapping d and t, 3 H, *o*- and *p*-H of Ph), 6.95 (t, 2 H, *J* 7.4, *m*-H of Ph), 6.05, 5.76, 5.71, 5.68 (4 × virtual q, 4 × 2 H, η-C$_5$*H*$_4$Pr^i), 3.30 (spt, 2 H, *J* 6.9, C*H*Me$_2$), 1.28, 1.21 (2 × d, 2 × 6 H, *J* 6.9, CH*Me*$_2$) ^{13}C-{^{1}H}:[l] 148.4 (μ-Ph*C*NH), 137.0 (*ipso*-C of Ph), 135.0 (*C*Pr^i), 126.7, 126.6, 126.0 (*o*-, *m*- and *p*-C of Ph), 114.2, 106.7, 101.0, 99.9 (4 × CH of η-*C*$_5$H$_4$Pr^i), 27.6 (*C*HMe$_2$), 22.7, 21.7 (CH*Me*$_2$)
18b[q]	Purple	26.7 (26.9)	2.4 (2.5)	1.5 (1.6)	27.6 (27.8)	^{1}H:[l,m] 10.35 (br s, 1 H, μ-PhCN*H*), 7.26 (overlapping d and t, 3 H, *o*- and *p*-H of Ph), 6.96 (t, 2 H, *J* 7.9, *m*-H of Ph), 5.86, 5.82, 5.74, 5.64 (4 × virtual q, 4 × 2 H, η-C$_5$*H*$_4$Me), 2.47 (s, 6 H, Me)

[a] Calculated values given in parentheses; halide = Cl or Br as appropriate. [b] At 25 °C in [$^2H_6$]benzene unless stated otherwise. Data given as: chemical shift (δ), multiplicity (s = singlet, d = doublet, t = triplet, q = quartet, spt = septet, m = multiplet, br = broad), relative intensity, coupling constant (in Hz) and assignment; for virtually coupled multiplets the apparent coupling constant is not given. For ^{1}H NMR spectra *J* refers to the ^{1}H–^{1}H coupling constant unless otherwise stated. [c] ν/cm^{-1}(KBr)(C≡O) 1969, 1934 or 1986, 1954 (CH$_2$Cl$_2$). [d] In [$^2H_6$]dichloromethane. [e] ν/cm^{-1}(C≡O)(KBr) 1970, 1943 and 1908. [f] ν/cm^{-1}(C≡O)(KBr) 2091 and 2051. [g] ν/cm^{-1}(C≡N)(KBr) 2193 and 1591. [h] ν/cm^{-1}(C≡N) 2188 and 1585. [i] At 203 K. [j] Analysis for **7b**·thf. [k] The oily solid was always contaminated with varying amounts of solvent. [l] In [$^2H_6$]dimethyl sulfoxide. [m] At 303 K. [n] ν/cm^{-1}(N–H)(KBr) 3118. [o] ν/cm^{-1}(N–H)(KBr) 3342. [p] ν/cm^{-1}(N–H)(KBr) 3344. [q] ν/cm^{-1}(N–H)(KBr) 3119.

Table 2 Selected bond lengths (Å) and angles (°) for [W$_2$(η-C$_5$H$_4$Me)$_2$Cl$_2$(μ-Cl)$_2$(CO)$_2$] **4b** with estimated standard deviations (e.s.d.s) in parentheses *

W(1)–W(1B)	2.9647(8)	W(1)–Cl(1)	2.446(4)
W(1)–Cl(1B)	2.513(4)	W(1)–Cl(2)	2.444(5)
W(1)–C(1)	1.99(2)	O(1)–C(1)	1.11(2)
W(1)–Cp$_{cent}$	1.98		
Cl(1)–W(1)–W(1B)	54.34(9)	Cl(1B)–W(1B)–W(1)	52.24(9)
Cl(1)–W(1)–Cl(1B)	74.8(2)	Cl(2)–W(1)–W(1B)	94.3(1)
Cl(2)–W(1)–Cl(1)	80.6(2)	Cl(2)–W(1)–Cl(1B)	146.1(1)
C(1)–W(1)–W(1B)	81.8(6)	C(1)–W(1)–Cl(1)	133.2(6)
C(1)–W(1)–Cl(1B)	91.8(6)	C(1)–W(1)–Cl(2)	88.3(6)
W(1)–Cl(1)–W(1B)	73.4(1)	O(1)–C(1)–W(1)	170.2(19)
Cp$_{cent}$–W(1)–C(1)	106.8	Cp$_{cent}$–W(1)–Cl(2)	105.2
Cp$_{cent}$–W(1)–Cl(1)	120.0	Cp$_{cent}$–W(1)–Cl(1B)	107.3

[W(1)–Cl(1)–Cl(1B) plane] to [W(1B)–Cl(1)–Cl(1B) plane] 97.7°

* Cp$_{cent}$ refers to the computed η-C$_5$H$_4$Me ring centroid.

Table 3 Fractional atomic coordinates for the non-hydrogen atoms of [W$_2$(η-C$_5$H$_4$Me)$_2$Cl$_2$(μ-Cl)$_2$(CO)$_2$] **4b** with e.s.d.s in parentheses

Atom	*x*	*y*	*z*
W(1)	0.069 89(3)	0.025(1)	0.148 03(4)
Cl(1)	−0.096 5(3)	0.201(1)	0.068 0(4)
Cl(2)	−0.053 9(4)	−0.163(1)	0.249 8(5)
O(1)	0.156(1)	−0.339(2)	0.055(2)
C(1)	0.125(2)	−0.203(3)	0.076(2)
C(2)	0.247(1)	0.058(4)	0.245(2)
C(3)	0.204(1)	−0.047(2)	0.340(2)
C(4)	0.132(1)	0.053(4)	0.402(2)
C(5)	0.130(1)	0.233(3)	0.348(2)
C(6)	0.199(1)	0.239(3)	0.249(2)
C(7)	0.068(2)	0.398(3)	0.386(3)

medium intensity at 1882 cm^{-1}, possibly indicative of a semi-bridging carbonyl ligand. The NMR data for the isomer of the ^{13}C-enriched **4a*** however (see above), suggest that the CO ligands of the second isomer are both predominantly terminally bound since only one set of ^{183}W satellites is observed whose intensity is of the incorrect magnitude for an atom bonded symmetrically to two W atoms. It was not possible to separate the two isomers of **4a** and **4b** by fractional crystallisation and the identity of the second isomer remains uncertain.

In contrast to the reaction of complex **1** with CO to give dinuclear products, toluene solutions of the bromide-supported analogue [W$_2$(η-C$_5$H$_4$Pr^i)$_2$Br$_4$] **2** react with CO to give the mononuclear derivative *fac*-[W(η-C$_5$H$_4$Pr^i)Br$_3$(CO)$_2$] **5** as the only isolable product in *ca.* 40% yield. Compound **5** was characterised by elemental analysis, IR and ^{1}H and ^{13}C NMR spectroscopy, and by a single-crystal X-ray diffraction analysis. The molecular structure is shown in Fig. 3, selected bond lengths and angles are given in Table 4, and fractional atomic coordinates for the non-hydrogen atoms are listed in Table 5.

Compound **5** exists as a monomer in the solid state. If the η-C$_5$H$_4$Pr^i ligand is considered to occupy a single co-ordination

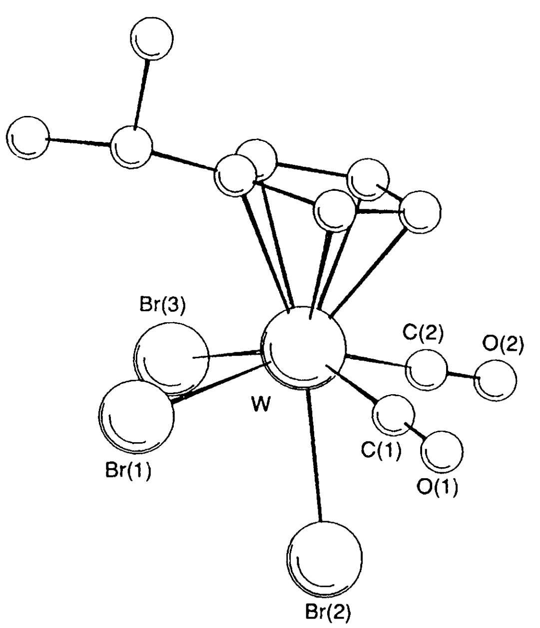

Fig. 3 Molecular structure of $[W(\eta\text{-}C_5H_4Pr^i)Br_3(CO)_2]$ **5**. Hydrogen atoms are omitted for clarity

Table 4 Selected bond lengths (Å) and angles (°) for $[W(\eta\text{-}C_5H_4Pr^i)Br_3(CO)_2]$ **5** with e.s.d.s in parentheses *

W–Br(1)	2.5918(8)	W–Br(2)	2.6350(8)
W–Br(3)	2.6114(9)	W–C(1)	2.046(9)
W–C(2)	2.037(9)	O(1)–C(1)	1.12(1)
O(2)–C(2)	1.14(1)	W–Cp_{cent}	2.00
Br(2)–W–Br(1)	81.27(3)	Br(3)–W–Br(1)	86.01(3)
Br(3)–W–Br(2)	82.08(3)	C(1)–W–Br(1)	83.2(2)
C(1)–W–Br(2)	71.7(2)	C(1)–W–Br(3)	152.9(2)
C(2)–W–Br(1)	152.1(2)	C(2)–W–Br(2)	71.4(2)
C(2)–W–Br(3)	84.8(3)	C(2)–W–C(1)	93.3(3)
O(1)–C(1)–W	179.2(7)	O(2)–C(2)–W	178.9(8)
Cp_{cent}–W–Br(1)	107.1	Cp_{cent}–W–Br(2)	167.5
Cp_{cent}–W–Br(3)	106.8	Cp_{cent}–W–C(1)	100.2
Cp_{cent}–W–C(2)	100.2		

* Cp_{cent} refers to the computed $\eta\text{-}C_5H_4Pr^i$ ring centroid.

Table 5 Fractional atomic coordinates for the non-hydrogen atoms of $[W(\eta\text{-}C_5H_4Pr^i)Br_3(CO)_2]$ **5** with e.s.d.s in parentheses

Atom	*x*	*y*	*z*
W	0.107 97(2)	0.789 41(2)	0.091 54(2)
Br(1)	−0.002 71(6)	0.742 69(5)	0.218 43(5)
Br(2)	0.030 50(7)	0.641 77(6)	0.021 99(6)
Br(3)	−0.066 46(8)	0.856 59(6)	0.016 42(7)
O(1)	0.251 1(6)	0.629 0(4)	0.162 7(5)
O(2)	0.199 6(6)	0.773 2(5)	−0.104 1(4)
C(1)	0.200 7(7)	0.685 7(6)	0.136 9(5)
C(2)	0.166 4(7)	0.778 1(6)	−0.034 0(6)
C(3)	0.210 0(8)	0.912 4(6)	0.058 1(6)
C(4)	0.276 1(7)	0.850 0(7)	0.105 1(6)
C(5)	0.231 8(6)	0.846 2(5)	0.193 2(5)
C(6)	0.144 1(5)	0.906 4(5)	0.199 9(5)
C(7)	0.129 2(7)	0.944 1(5)	0.116 0(6)
C(8)	0.087 1(6)	0.932 1(5)	0.283 4(6)
C(9)	−0.021 5(7)	0.980 3(6)	0.271 5(7)
C(10)	0.167 1(8)	0.987 6(6)	0.338 6(6)

site, the molecular structure may be described as pseudo-octahedral with two *cis*-Br and *cis*-CO ligands in the equatorial plane and with the $\eta\text{-}C_5H_4Pr^i$ ring *trans* to a further Br ligand. The tungsten atom lies *ca.* 0.54 Å out of the plane containing the equatorial Br and CO ligands. The Cp_{cent}–W–Br(2) angle (167.5°) is substantially less than 180° with Br(2) displaced towards the two CO ligands, presumably reflecting steric effects.

The parent compounds $[M(\eta\text{-}C_5H_5)X_3(CO)_2]$ (M = Mo or W, X = Cl or Br) are well known but have not been characterised crystallographically.[13] The IR and ^1H and ^{13}C NMR data (Table 1) of complex **5** are consistent with the solid-state structure and are analogous to those described previously for the parent complexes $[M(\eta\text{-}C_5H_5)X_3(CO)_2]$.

The differing reactivities of complexes **1** and **2** with CO to give di- and mono-nuclear products respectively may be associated in part with the differences in W–X bond lengths for X = Cl or Br.[14] Thus for a given W–X–W angle in the $W_2(\mu\text{-}X)_2$ core the W–W bond length would be substantially longer for the bromide than for the chloride analogue leading in turn to diminished metal–metal bonding.

Reaction with tert-*Butyl Isocyanide.*—Since the CO and RNC ligands are related in their σ-donor and π-acceptor characteristics, we were interested to explore the reactivity of complex **1** towards isocyanides RNC.

Treatment of a diethyl ether solution of complex **1** with Bu^tNC for 12 h afforded purple crystals of $[W_2(\eta\text{-}C_5H_4R)_2Cl_3(\mu\text{-}Cl)(\mu\text{-}\sigma{:}\eta^2\text{-}Bu^tNC)(Bu^tNC)]$ (R = Pr^i **6a** or Me **6b**) in *ca.* 75–80% yield. Compounds **6** were characterised by elemental analysis and by IR and ^1H and ^{13}C NMR spectroscopy. It was not possible to obtain crystals suitable for a single-crystal diffraction analysis. The analytical data for **6** are consistent with the repeat formula $[W(\eta\text{-}C_5H_4R)Cl_2(Bu^tNC)]_x$. The IR spectra show bands at *ca.* 2190 and 1590 cm^{-1}, consistent with the presence of terminal and bridging Bu^tNC ligands.[15] The ^1H and ^{13}C NMR spectra show resonances assignable to two types of diastereotopic $\eta\text{-}C_5H_4R$ moieties, and to two Bu^t groups. Two additional resonances at δ *ca.* 232 and 146 in the ^{13}C NMR spectra are assigned to the terminal carbon atoms of the Bu^tNC ligands; the low-field resonance for compound **6b** shows ^{183}W satellites of the correct intensity for a carbon atom bonded equivalently to two tungsten atoms [$^1J(^{183}W\text{-}^{13}C)$ = 155 Hz, satellites *ca.* 26% of total signal intensity]. The chemical shifts for terminal and bridging isocyanide ligands generally lie in the range δ 140–170 and > 200 respectively.[16–18]

The ^{13}C NMR data in Table 1 do not uniquely define the precise mode of co-ordination of the bridging Bu^tNC ligand (shown as two possible representations **A** and **B** below). Both modes require that the two $^1J(^{13}C\text{-}^{183}W)$ coupling constants are equivalent within the resolution of the ^{13}C NMR experiment (*ca.* 1.5 Hz). For **B** there is the possibility of equivalence of two different $^1J(^{13}C\text{-}^{183}W)$ coupling constants *via* a low-activation-energy fluxional process. Mode **A** may not be eliminated *a priori* and models for **A** and **B** have been structurally characterised previously for isocyanide ligands bridging two metal atoms.[16,19] Mode **B** may, however, be the more likely based on the crystallographically determined structure of $[W_2(\eta\text{-}C_5H_4Me)_2Cl_3(\mu\text{-}Cl)(\mu\text{-}\sigma{:}\eta^2\text{-}EtCN)]$ **11b** (see below) and we have preferred to show this structure in Scheme 1.

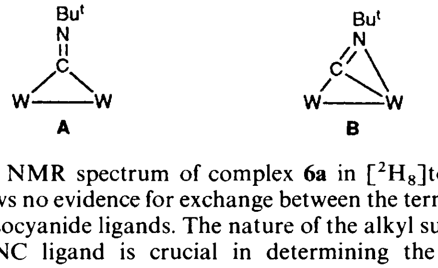

The ^1H NMR spectrum of complex **6a** in $[^2H_8]$toluene at 90 °C shows no evidence for exchange between the terminal and bridging isocyanide ligands. The nature of the alkyl substituent of the RNC ligand is crucial in determining the reaction products with **1** since reaction with isocyanide ligands having R other than Bu^t affords only complex mixtures.

Reaction with $[N(PPh_3)_2]Cl$.—Addition of 1 equivalent of $[N(PPh_3)_2]Cl$ to complex **1** in dichloromethane affords the

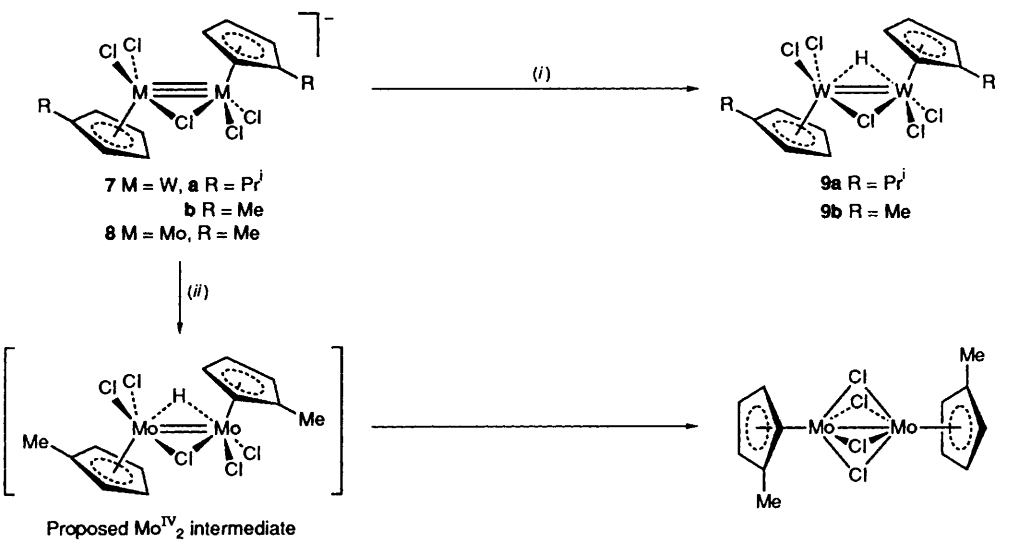

Scheme 2 *Reagents and conditions*: (*i*) (for M = W, R = Pr^i or Me) HCl (g), toluene, >90%; (*ii*) (for M = Mo, R = Me) HCl (g), toluene, >90%; $[N(PPh_3)_2]^+$ cations for **7** and **8** are not illustrated

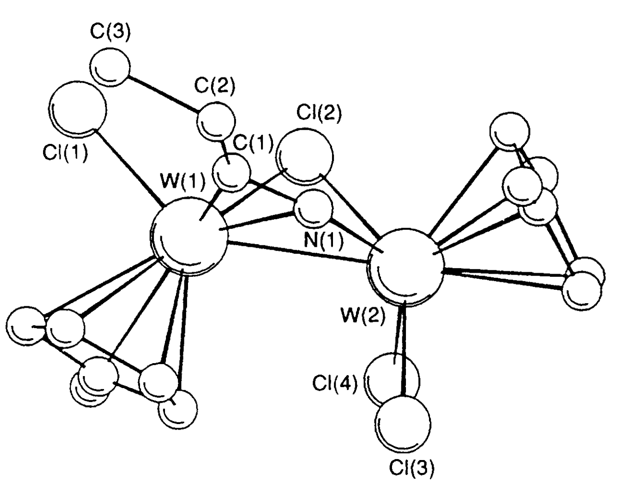

Fig. 4 Molecular structure of $[W_2(\eta\text{-}C_5H_4Me)_2Cl_3(\mu\text{-}Cl)(\mu\text{-}\sigma:\eta^2\text{-}EtCN)]$ **11b**. Hydrogen atoms are omitted for clarity

Table 6 Selected bond lengths (Å) and angles (°) for $[W_2(\eta\text{-}C_5H_4Me)_2Cl_3(\mu\text{-}Cl)(\mu\text{-}\sigma:\eta^2\text{-}EtCN)]$ **11b** with e.s.d.s in parentheses *

W(1)–W(2)	2.8986(6)	W(1)–Cl(1)	2.390(3)
W(1)–Cl(2)	2.432(3)	W(1)–N(1)	2.070(8)
W(1)–C(1)	1.98(1)	W(2)–Cl(2)	2.421(3)
W(2)–Cl(3)	2.429(3)	W(2)–Cl(4)	2.424(3)
W(2)–N(1)	1.948(7)	N(1)–C(1)	1.30(1)
C(1)–C(2)	1.49(1)	C(2)–C(3)	1.51(2)
W(1)–$Cp_{cent(1)}$	2.01	W(1)–$Cp_{cent(2)}$	2.00
Cl(1)–W(1)–W(2)	131.92(8)	Cl(2)–W(1)–W(2)	53.16(6)
Cl(2)–W(1)–Cl(1)	79.9(1)	N(1)–W(1)–W(2)	42.2(2)
N(1)–W(1)–Cl(1)	124.8(2)	N(1)–W(1)–Cl(2)	76.6(2)
C(1)–W(1)–W(2)	79.6(3)	C(1)–W(1)–Cl(1)	102.0(3)
C(1)–W(1)–Cl(2)	100.4(3)	C(1)–W(1)–N(1)	37.4(4)
Cl(2)–W(2)–W(1)	53.49(7)	Cl(3)–W(2)–W(1)	94.12(7)
Cl(3)–W(2)–Cl(2)	144.0(1)	Cl(4)–W(2)–W(1)	93.23(7)
Cl(4)–W(2)–Cl(2)	83.0(1)	Cl(4)–W(2)–Cl(3)	84.0(1)
N(1)–W(2)–W(1)	45.5(2)	N(1)–W(2)–Cl(2)	79.1(2)
N(1)–W(2)–Cl(3)	88.4(2)	N(1)–W(2)–Cl(4)	137.4(2)
W(2)–Cl(2)–W(1)	73.35(7)	W(2)–N(1)–W(1)	92.3(3)
C(1)–N(1)–W(1)	67.4(6)	C(1)–N(1)–W(2)	159.4(7)
N(1)–C(1)–W(1)	75.2(6)	C(2)–C(1)–W(1)	154.0(8)
C(2)–C(1)–N(1)	130.7(10)		

* $Cp_{cent(1)}$ and $Cp_{cent(2)}$ refer to the computed $\eta\text{-}C_5H_4Me$ ring centroids for W(1) and W(2) respectively.

salts $[N(PPh_3)_2][W_2(\eta\text{-}C_5H_4R)_2Cl_4(\mu\text{-}Cl)]$ (R = Pr^i **7a** or Me **7b**) in quantitative yields (Scheme 1). Compounds **7** were characterised by elemental analysis and by ^1H and ^{13}C NMR spectroscopy. The room-temperature ^1H and ^{13}C NMR spectra of **7** show resonances assignable to the $[N(PPh_3)_2]^+$ cation and to one type of $\eta\text{-}C_5H_4R$ moiety, the ring protons of which appear as a pair of mutually coupled AA′BB′ virtual triplets. However, the NMR spectra of cold (198 K) $[^2H_2]$dichloromethane solutions of **7** show resonances assignable to a single *diastereotopic* $\eta\text{-}C_5H_4R$ ligand, the ring protons appearing as four mutually coupled virtual quartets (an ABCD spin system) in the ^1H NMR spectrum (Table 1). On the basis of these data we propose that compounds **7** are fluxional at room temperature but have the chloride-bridged ground-state structure shown in Scheme 1, analogous to that of the structurally characterised anion $[Mo_2(\eta\text{-}C_5H_5)_2Cl_4(\mu\text{-}Cl)]^-$ recently reported by Poli and Rheingold.[20]

The reported NMR data for $[Mo_2(\eta\text{-}C_5H_5)_2Cl_4(\mu\text{-}Cl)]^-$ do not allow us to determine if this complex is also fluxional since the unsubstituted $\eta\text{-}C_5H_5$ ligand is not prochiral. We therefore prepared the corresponding ring-substituted dimolybdenum species $[N(PPh_3)_2][Mo_2(\eta\text{-}C_5H_4Me)_2Cl_4(\mu\text{-}Cl)]$ **8** from $[Mo_2(\eta\text{-}C_5H_4Me)_2(\mu\text{-}Cl)_4]^2$ and $[N(PPh_3)_2]Cl$. The NMR data for **8** show that this compound is also fluxional with the ring protons appearing as a pair of AA′BB′ triplets at room temperature and as four mutually coupled virtual quartets in the low-temperature (slow-exchange) limit (203 K). It is likely therefore that the ring-unsubstituted species $[Mo_2(\eta\text{-}C_5H_5)_2Cl_4(\mu\text{-}Cl)]^-$ is also fluxional and that complexes **7** and **8** have analogous ground-state structures.

The nature of the fluxional process in complexes **7** and **8** is not well established, but the NMR data are consistent with a mechanism which essentially involves rotation of the μ-chloro ligand around the metal–metal vector. Values for the free energy of activation ($\Delta G^\ddagger$) for the fluxional process in **7a** and **8** have been determined from NMR coalescence studies since $\Delta G^\ddagger = 4.573T_c[9.972 \log_{10}(T_c/\delta_v)]$ where T_c is the coalescence temperature and δ_v is the frequency separation of the two exchanging resonances in the slow-exchange limit.[21] For $[W_2(\eta\text{-}C_5H_4Pr^i)_2Cl_4(\mu\text{-}Cl)]^-$ **7a** $\Delta G^\ddagger = 11.4 \pm 0.5$ kcal mol^{-1} (at 248 K) and for $[Mo_2(\eta\text{-}C_5H_4Me)_2Cl_4(\mu\text{-}Cl)]^-$ **8** $\Delta G^\ddagger = 10.5 \pm 0.5$ kcal mol^{-1} (at 243 K).

The ditungsten anions $[W_2(\eta\text{-}C_5H_4R)_2Cl_4(\mu\text{-}Cl)]^-$ are readily protonated on treatment with HCl gas in toluene to afford the previously described μ-hydrido derivatives $[W_2(\eta\text{-}$

Table 7 Fractional atomic coordinates for the non-hydrogen atoms of [$W_2(\eta\text{-}C_5H_4Me)_2Cl_3(\mu\text{-}Cl)(\mu\text{-}\sigma:\eta^2\text{-}EtCN)$] **11b** with e.s.d.s in parentheses

Atom	*x*	*y*	*z*
W(1)	0.885 36(5)	0.157 07(4)	0.299 56(3)
W(2)	0.806 57(5)	0.322 03(4)	0.146 75(3)
Cl(1)	0.767 4(5)	−0.079 3(3)	0.284 2(3)
Cl(2)	0.719 9(4)	0.070 3(3)	0.095 7(2)
Cl(3)	1.030 6(4)	0.526 8(3)	0.268 6(3)
Cl(4)	1.036 7(4)	0.264 9(3)	0.041 6(2)
N(1)	0.737(1)	0.305 3(8)	0.290 8(7)
C(1)	0.721(1)	0.258(1)	0.378 5(8)
C(2)	0.619(1)	0.296(1)	0.473(1)
C(3)	0.597(2)	0.187(1)	0.535(1)
C(11)	1.125(2)	0.098(1)	0.413(1)
C(12)	1.180(2)	0.126(1)	0.312(1)
C(13)	1.172(1)	0.265(1)	0.324(1)
C(14)	1.112(1)	0.321(1)	0.429(1)
C(15)	1.083(2)	0.220(1)	0.480(1)
C(16)	1.239(2)	0.028(1)	0.217(1)
C(21)	0.599(2)	0.459(1)	0.145(1)
C(22)	0.524(1)	0.317(1)	0.075(1)
C(23)	0.602(2)	0.283(1)	−0.022(1)
C(24)	0.727(2)	0.409(1)	−0.015(1)
C(25)	0.719(2)	0.509(1)	0.084(1)
C(26)	0.545(2)	0.539(1)	0.255(1)

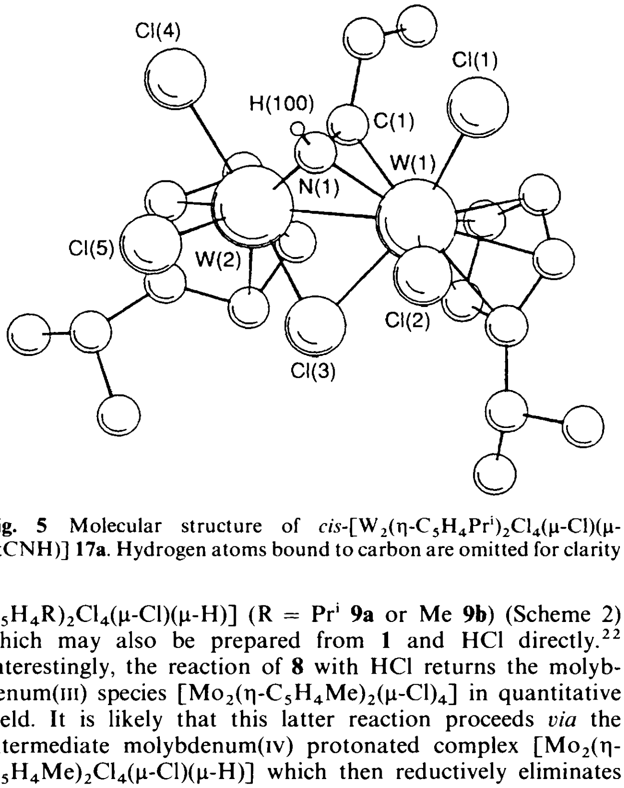

Fig. 5 Molecular structure of *cis*-[$W_2(\eta\text{-}C_5H_4Pr^i)_2Cl_4(\mu\text{-}Cl)(\mu\text{-}EtCNH)$] **17a**. Hydrogen atoms bound to carbon are omitted for clarity

$C_5H_4R)_2Cl_4(\mu\text{-}Cl)(\mu\text{-}H)$] (R = Pr^i **9a** or Me **9b**) (Scheme 2) which may also be prepared from **1** and HCl directly.[22] Interestingly, the reaction of **8** with HCl returns the molybdenum(III) species [$Mo_2(\eta\text{-}C_5H_4Me)_2(\mu\text{-}Cl)_4$] in quantitative yield. It is likely that this latter reaction proceeds *via* the intermediate molybdenum(IV) protonated complex [$Mo_2(\eta\text{-}C_5H_4Me)_2Cl_4(\mu\text{-}Cl)(\mu\text{-}H)$] which then reductively eliminates HCl. We note that although the μ-dihydride derivative [$W_2(\eta\text{-}C_5H_4Pr^i)_2Cl_4(\mu\text{-}H)_2$] reductively eliminates H_2 on warming in solution,[4] compounds **9** appear to show no tendency to eliminate HCl. The relative stabilities of [$M_2(\eta\text{-}C_5H_4R)_2Cl_4(\mu\text{-}Cl)(\mu\text{-}H)$] (where M = W) and [$M_2(\eta\text{-}C_5H_4Me)_2Cl_4(\mu\text{-}Cl)(\mu\text{-}H)$] (M = Mo) are consistent with the accepted view that tungsten generally supports higher oxidation states relative to those supported by molybdenum.[23]

Reaction with Nitriles R′CN.—Treatment of light petroleum suspensions of complex **1** with an excess of P_2O_5-dried nitriles R′CN (R′ = Me, Et or Ph) affords the highly moisture-sensitive complexes [$W_2(\eta\text{-}C_5H_4R)_2Cl_3(\mu\text{-}Cl)(\mu\text{-}\sigma:\eta^2\text{-}R'CN)$] (R′ = Me **10**, Et **11** or Ph **12**); R = Pr^i **a** or Me **b**. Compounds **10–12** were characterised by ^1H and ^{13}C NMR spectroscopy, and for **11b** a single-crystal X-ray structure determination was carried out.

The molecular structure of [$W_2(\eta\text{-}C_5H_4Me)_2Cl_3(\mu\text{-}Cl)(\mu\text{-}\sigma:\eta^2\text{-}EtCN)$] **11b** is shown in Fig. 4, selected bond lengths and angles are given in Table 6, and fractional atomic coordinates for the non-hydrogen atoms are listed in Table 7. Compound **11b** contains a W–W bond of length 2.8986(6) Å bridged by a Cl and a EtCN ligand. The EtCN moiety is bound in a σ fashion to W(2) and in a dihapto (η^2) fashion to W(1), with the N atom binding more tightly to W(2) [N(1)–W(2) 1.948(7) Å] than to W(1) [N(1)–W(1) 2.070(8) Å]. The N(1)–C(1) bond length [1.30(1) Å] approaches that of a N=C double bond (typical value *ca.* 1.28 Å) implying substantial back donation of electron density from the dimetal centre to the vacant π* orbitals of the μ-nitrile ligand.

The ^1H and $^{13}C\text{-}\{^1H\}$ NMR spectra of complexes **10–12** show resonances assignable to two diastereotopic $\eta\text{-}C_5H_4R$ ligands and to a co-ordinated R′CN ligand. In addition, the $^{13}C\text{-}\{^1H\}$ NMR spectra reveal resonances for the internal carbon atoms of the R′CN ligand at δ *ca.* 240 which possess ^{183}W satellites (where observed) of the proper intensity for a carbon atom bonded to one tungsten atom [$^1J(^{13}C\text{-}^{183}W)$ *ca.* 95 Hz; *ca.* 14% of total signal intensity]. There is no evidence for a ν(C≡N) absorption in the IR spectra of **10–12** consistent with the significant decrease in C–N bond order suggested by the lengthened C–N bond distance. Complexes containing a μ-(σ:η^2)-nitrile moiety have been reported previously.[24]

Reaction of [$W_2(\eta\text{-}C_5H_4R)_2Cl_3(\mu\text{-}Cl)(\mu\text{-}\sigma:\eta^2\text{-}R'CN)$] *with* HCl: *Synthesis of cis and trans*-[$W_2(\eta\text{-}C_5H_4R)_2Cl_4(\mu\text{-}Cl)(\mu\text{-}R'CNH)$] (R′ = Me, Et *or* Ph; R = Pr^i *or* Me).—Treatment of diethyl ether solutions of [$W_2(\eta\text{-}C_5H_4R)_2Cl_3(\mu\text{-}Cl)(\mu\text{-}\sigma:\eta^2\text{-}R'CN)$] **10–12** with HCl gas (1 atm) for a few minutes afforded near-quantitative yields of orange solids analysing as [$W_2(\eta\text{-}C_5H_4R)_2Cl_4(R'CN)(HCl)$] (R′ = Me **13**, Et **14** or Ph **15**; R = Pr^i **a** or Me **b**). Compounds **13–15** were characterised by elemental analysis and by ^1H and ^{13}C NMR spectroscopy, and also by comparison with the crystallographically characterised isomer, *cis*-[$W_2(\eta\text{-}C_5H_4Pr^i)_2Cl_4(\mu\text{-}Cl)(\mu\text{-}EtCNH)$] (see below).

The ^1H and $^{13}C\text{-}\{^1H\}$ NMR spectra of the compounds **13–15** show resonances assignable to two types of diastereotopic $\eta\text{-}C_5H_4R$ ligands and to a R′ group. An additional resonance appears at δ *ca.* 140 for all of the orange compounds. In the ^1H NMR spectra of **14** the Et group is diastereotopic. In addition, all of the ^1H NMR spectra of [$^2H_6$]dimethyl sulfoxide solutions of **13–15** show a broad, low-field resonance at δ *ca.* 11 integrating as one proton per R′ group. This latter band is virtually absent in the ^1H NMR spectrum of the corresponding isotopomer **14a-d** prepared from [$W_2(\eta\text{-}C_5H_4Pr^i)_2Cl_3(\mu\text{-}Cl)(\mu\text{-}\sigma:\eta^2\text{-}EtCN)$] **11a** and DCl gas. Furthermore, the IR spectra of **14a–d** showed a new band of strong intensity at 2314 cm^{-1} and the original band observed at 3118 cm^{-1} for **14a** was much reduced in intensity.

Dissolving the orange complexes in dichloromethane for 30 min afforded the red-purple complexes *cis*-[$W_2(\eta\text{-}C_5H_4R)_2Cl_4(\mu\text{-}Cl)(\mu\text{-}R'CNH)$] (R′ = Me **16**, Et **17** or Ph **18**; R = Pr^i **a** or Me **b**) in quantitative yield. Elemental analyses for the compounds **16–18** showed them to have essentially identical empirical formulae to those of their respective precursors **13–15**; they were further characterised by IR and ^1H and ^{13}C NMR spectroscopy. Compound **17a** has been structurally characterised by a single-crystal X-ray diffraction analysis,[3] and the molecular structure is shown in Fig. 5.

Compound **17a** consists of two mutually eclipsed $W(\eta\text{-}C_5H_4Pr^i)Cl_2$ fragments linked by bridging Cl and EtCNH groups. If the $\eta\text{-}C_5H_4Pr^i$ rings are considered to occupy a single co-ordination site and any metal–metal bond is ignored then the compound may be described as a confacial bioctahedron. The W–W bond length [2.9359(4) Å] is substantially lengthened from that of $[W_2(\eta\text{-}C_5H_4Pr^i)_2Cl_4]$ **1a** [W≡W 2.3678(6) Å].[2] The C–N bond length [1.405(8) Å] is notably longer than those observed for η^2-RCNR′ complexes (typically 1.22–1.30 Å).[25] These observations suggest extensive donation of electron density from the tungsten centre to vacant π^* orbitals of the μ-EtCNH ligand in a manner analogous to that proposed to occur for dinuclear μ-alkyne complexes.[26]

The solution ^1H and ^{13}C NMR spectral data for complexes **16**–**18** are consistent with the maintenance of structures analogous to that of **17a** in the solid state. Thus, the ^1H NMR spectra shows resonances assignable to one type of diastereotopic $\eta\text{-}C_5H_4R$ ring and to a R′CNH ligand, the N–H resonance appearing as a broad signal at δ *ca.* 6 (in $[^2H_2]$-dichloromethane) or δ *ca.* 10 (in $[^2H_6]$dimethyl sulfoxide). This band is virtually absent for the isotopomer $[W_2(\eta\text{-}C_5H_4Pr^i)_2Cl_4(\mu\text{-}Cl)(\mu\text{-}MeCND)]$ **16a**–**d**. For the μ-EtCNH compounds **17a** the H_a and H_b protons of the $CH_3CH_aH_bCNH$ ligand are equivalent and appear as a quartet in the ^1H NMR spectrum (Table 1). The $^{13}C\text{-}\{^1H\}$ NMR spectra show resonances assignable to $\eta\text{-}C_5H_4R$ and R′ moieties. An additional singlet at δ *ca.* 145, which (where observed) shows ^{183}W satellites of the proper intensity for a carbon atom bonded to two tungsten atoms, is assigned to the internal carbon atom of the μ-R′CNH ligand. A sharp band at *ca.* 3340 cm^{-1} in the IR spectra of **16**–**18** is assigned as ν(N–H); the isotopomer *cis*-$[W_2(\eta\text{-}C_5H_4Pr^i)_2Cl_4(\mu\text{-}Cl)(\mu\text{-}MeCND)]$ **16a**–**d** shows a band assignable to ν(N–D) at 2486 cm^{-1}.

From the data described above and in Table 1, the first-formed orange (kinetic) products **13**–**15** are assigned the *trans*-$[W_2(\eta\text{-}C_5H_4R)_2Cl_4(\mu\text{-}Cl)(\mu\text{-}R'CNH)]$ structures shown in Scheme 1. For instance, the ^1H NMR spectra of **13**–**15** and **16**–**18** all show bands assignable to an NH resonance and the chemical shifts of the internal quaternary carbon atoms of the μ-R′CNH ligand are similar for all of these complexes. The lack of a molecular mirror plane perpendicular to the W–W vector in the *trans* isomers **13**–**15** is evidenced by the presence of two $\eta\text{-}C_5H_4R$ ring environments in their NMR spectra and by the diastereotopic methylene linkage of the Et groups in **14**.

Another possible interpretation of the data for the orange compounds could be the salts $[W_2(\eta\text{-}C_5H_4R)_2Cl_4(\mu\text{-}R'CNH)]^+Cl^-$. If this were the case, then it should be possible to synthesise other salts such as $[W_2(\eta\text{-}C_5H_4R)_2Cl_4(\mu\text{-}RCNH)]^+[BF_4]^-$. However, treatment of a toluene solution of complex **11a** with HBF_4 in ether (*ca.* 1 mol dm^{-3}) gave only a complex mixture as shown by ^1H NMR spectroscopy.

Although the RCNR′ (iminoacyl) ligand has been found to co-ordinate to mononuclear complexes in a dihapto fashion and to trinuclear complexes in a $\sigma:\sigma:\eta^2$ fashion, to our knowledge complex **17a** is the first structurally characterised example of a $\mu\text{-}\eta^2:\eta^2$-co-ordinated RCNR′ ligand. The μ-iminoacyl complexes described here are clearly related to other perpendicular ($\mu\text{-}\eta^2:\eta^2$) bridge complexes of the general type $L_nM(\mu\text{-}\eta^2:\eta^2\text{-}RCX)ML_n$ (X = CR, O, P or S).[27]

Experimental

All manipulations of air- and moisture-sensitive materials were performed using either standard Schlenk-line techniques under an atmosphere of dinitrogen, which had been purified by passage over BASF catalyst and 4 Å molecular sieves, or in an inert-atmosphere dry-box containing dinitrogen. Solvents were pre-dried by standing over 4 Å molecular sieves and then distilled under an atmosphere of dinitrogen from phosphorus pentaoxide (dichloromethane), sodium (toluene), potassium–benzophenone [thf (tetrahydrofuran)], or sodium–potassium alloy (1:3 w/w) [light petroleum (b.p. 40–60 °C), diethyl ether]. Deuteriated solvents for NMR studies were stored in Young's ampoules under an atmosphere of dinitrogen over sodium–potassium alloy ($[^2H_6]$benzene, $[^2H_8]$toluene) or molecular sieves ($[^2H_2]$dichloromethane, $[^2H_6]$dimethyl sulfoxide). The nitriles MeCN, EtCN and PhCN were dried by distilling from P_2O_5 before use; Bu^tNC was used as received (Aldrich).

Proton, $^{13}C\text{-}\{^1H\}$ and $^{31}P\text{-}\{^1H\}$ NMR spectra were recorded on a Brüker AM 300 spectrometer, (^1H, 300; ^{13}C, 75.5; ^{31}P, 121.6 MHz). Spectra were referenced internally using the residual protio solvent (^1H) and solvent (^{13}C) resonances relative to tetramethylsilane (δ 0), or externally using trimethyl phosphate in $[^2H_2]$water (^{31}P). All chemical shifts are quoted in δ and coupling constants are in Hz. Infrared spectra were recorded as KBr disks or as a CH_2Cl_2 solution in a NaCl cell using a Perkin-Elmer 1510 FT interferometer. Elemental analyses were performed by the analytical department of this laboratory. The compounds $[W_2(\eta\text{-}C_5H_4R)_2X_4]$ (X = Cl, R = Pr^i or Me; X = Br, R = Pr^i) were prepared as described previously.[2]

Preparation of $[W_2(\eta\text{-}C_5H_4Me)_2Cl_2(\mu\text{-}Cl)_2(dmpe)]$ **3**.—A solution of $[W_2(\eta\text{-}C_5H_4Me)_2Cl_4]$ (230 mg, 0.34 mmol) in toluene (25 cm^3) was treated with dmpe (110 mg, 0.70 mmol) in light petroleum (6 cm^3) to give a dark red solution which, on standing (12 h), deposited dark red crystals of complex **3** and a small quantity of a flocculent brown powder. The crystals were isolated by decanting the brown powder and supernatant as a slurry and washing with toluene (2 × 5 cm^3) and light petroleum (10 cm^3). Yield: 65 mg (23%).

Preparation of $[W_2(\eta\text{-}C_5H_4R)_2Cl_2(\mu\text{-}Cl)_2(CO)_2]$ (R = Pr^i **4a** *or* Me **4b**).—Carbon monoxide gas was bubbled through a solution of $[W_2(\eta\text{-}C_5H_4R)_2Cl_4]$ in toluene (*ca.* 20 cm^3) for 5 min at room temperature to give a red-brown solution which was allowed to stand under an atmosphere of CO. After 12 h a red-brown precipitate formed. The supernatant was decanted and the residues were washed with light petroleum (2 × 10 cm^3) and dried *in vacuo* to afford brown microcrystals of $[W_2(\eta\text{-}C_5H_4Pr^i)_2Cl_2(\mu\text{-}Cl)_2(CO)_2]$ **4a**. Yield: 190 mg (90%). The complex $[W_2(\eta\text{-}C_5H_4Me)_2Cl_2(\mu\text{-}Cl)_2(CO)_2]$ **4b** was prepared in a similar manner (yield: 90%).

Preparation of $[W(\eta\text{-}C_5H_4Pr^i)Br_3(CO)_2]$ **5**.—Carbon monoxide gas was bubbled through a solution of $[W_2(\eta\text{-}C_5H_4Pr^i)_2Br_4]$ (300 mg, 0.33 mmol) in toluene (*ca.* 20 cm^3) for 5 min at r.t. to give a yellow solution which was allowed to stand under an atmosphere of CO. After 12 h a yellow precipitate formed. The supernatant was decanted and the residues washed with light petroleum (2 × 10 cm^3) and dried *in vacuo* to afford yellow microcrystals of $[W(\eta\text{-}C_5H_4Pr^i)Br_3(CO)_2]$ **5**. Yield: *ca.* 40%.

Preparation of $[W_2(\eta\text{-}C_5H_4R)_2Cl_3(\mu\text{-}Cl)(\mu\text{-}\sigma:\eta^2\text{-}Bu^tNC)(Bu^tNC)]$ (R = Pr^i **6a** *or* Me **6b**).—A suspension of $[W_2(\eta\text{-}C_5H_4Pr^i)_2Cl_4]$ (200 mg, 0.27 mmol) in diethyl ether (*ca.* 20 cm^3) was treated with an excess of Bu^tNC (2 cm^3 of 0.3 mol dm^{-3} solution in toluene) at r.t. The mixture was stirred for 12 h to give a red-purple precipitate. The supernatant was decanted and the residues washed with light petroleum (2 × 10 cm^3) and dried *in vacuo*. Subsequent recrystallisation from toluene–light petroleum afforded red-purple microcrystals of $[W_2(\eta\text{-}C_5H_4Pr^i)_2Cl_3(\mu\text{-}Cl)(\mu\text{-}\sigma:\eta^2\text{-}Bu^tNC)(Bu^tNC)]$ **6a**. Yield: 80%. The homologue $[W_2(\eta\text{-}C_5H_4Me)_2Cl_3(\mu\text{-}Cl)(\mu\text{-}\sigma:\eta^2\text{-}Bu^tNC)(Bu^tNC)]$ **6b** was prepared by a similar route but with recrystallisation from a mixture of diethyl ether and light petroleum. Yield 75%.

Preparation of $[N(PPh_3)_2][W_2(\eta\text{-}C_5H_4R)_2Cl_4(\mu\text{-}Cl)]$ (R = Pr^i **7a** *or* Me **7b**).—A slight excess of $[W_2(\eta\text{-}C_5H_4Pr^i)_2Cl_4]$ (200 mg, 0.27 mmol) and $[N(PPh_3)_2]Cl$ (143 mg, 0.25 mmol) were dissolved in CH_2Cl_2 (15 cm^3) at room temperature. After 1 h the volatiles were removed under reduced pressure. The residue was washed with toluene (2 × 10 cm^3) {to remove the excess $[W_2(\eta\text{-}C_5H_4Pr^i)_2Cl_4]$} and light petroleum (2 × 10 cm^3) and dried *in vacuo* to give the analytically pure product $[N(PPh_3)_2][W_2(\eta\text{-}C_5H_4Pr^i)_2Cl_4(\mu\text{-}Cl)]$ **7a**. Yield: 80%. The complex $[N(PPh_3)_2]$-$[W_2(\eta\text{-}C_5H_4Me)_2Cl_4(\mu\text{-}Cl)]$ **7b** was prepared in a similar

Table 8 Crystal data, data collection and processing parameters for $[W_2(\eta\text{-}C_5H_4Me)_2Cl_2(\mu\text{-}Cl)_2(CO)_2]$ **4b**, $[W(\eta\text{-}C_5H_4Pr^i)Br_3(CO)_2]$ **5** and $[W_2(\eta\text{-}C_5H_4Me)_2Cl_3(\mu\text{-}Cl)(\mu\text{-}\sigma:\eta^2\text{-}EtCN)]$ **11b**

	4b	**5**	**11b**
Formula	$C_{14}H_{14}Cl_4O_2W_2$	$C_{10}H_{11}Br_3O_2W$	$C_{15}H_{19}Cl_4NW_2$
M	723.78	576.68	722.84
Crystal size/mm	0.20 × 0.30 × 0.55	0.20 × 0.30 × 0.60	Irregular
Crystal system	Monoclinic	Orthorhombic	Triclinic
Space group	*C*2	*Pbca*	$P\bar{1}$
a/Å	12.674(3)	12.162(2)	7.882(1)
b/Å	7.342(1)	15.061(3)	10.222(1)
c/Å	9.495(2)	15.151(3)	12.079(7)
α/°	90	90	106.75(6)
β/°	103.07(2)	90	99.04(9)
γ/°	90	90	99.14(11)
U/Å³	860.7	2775.3	898.7
Z	2	8	2
D_c/g cm⁻³	2.793	2.76	2.67
μ/cm⁻¹	142.8	170.5	136.7
F(000)	660	2048	664
2θ limits/°	2–52	2–50	3–48
ω scan width (+0.35 tanθ)/°	0.90	1.0	1.30
Total data collected	1098	2875	3343
Total unique data	913	2435	2818
No. of observations $[I > 3\sigma(I)]$	867	1687	2353
R(merge)	0.053	0.028	0.063
No of variables	101	146	195
Observations, variables	8.6	11.6	12.1
Weighting coefficients	5.07, 22.2	30.5, −32.4, 20.4	54.1, −46.9, 38.6
Maximum peak in final difference map/e Å⁻³	0.82	0.73	1.4 [1.4 Å from W(1)]
R^a	0.035	0.025	0.040
R'^b	0.041	0.030	0.048

[a] $R = \Sigma||F_o| - |F_c||/\Sigma|F_o|$. [b] $R' = [\Sigma(|F_o| - |F_c|)^2/\Sigma|F_o|^2]^{\frac{1}{2}}$.

manner and was recrystallised from a thf–diethyl ether mixture as dark green microcrystals which contained one molecule of thf per formula unit. Yield: 95%.

Preparation of $[N(PPh_3)_2][Mo_2(\eta\text{-}C_5H_4Me)_2Cl_4(\mu\text{-}Cl)]$ **8**—. The compound $[N(PPh_3)_2]Cl$ (290 mg, 0.5 mmol) and a slight excess of $[Mo_2(\eta\text{-}C_5H_4Me)_2(\mu\text{-}Cl)_4]$ (250 mg, 0.51 mmol) were dissolved in CH_2Cl_2 (15 cm³) at room temperature. After 12 h the volatiles were removed under reduced pressure. The residue was washed with toluene (2 × 10 cm³) and light petroleum (2 × 10 cm³) and dried *in vacuo* to give the analytically pure product $[N(PPh_3)_2][Mo_2(\eta\text{-}C_5H_4Me)_2Cl_4(\mu\text{-}Cl)]$ **8**. Yield: 90%.

Reaction of $[N(PPh_3)_2][W_2(\eta\text{-}C_5H_4R)_2Cl_4(\mu\text{-}Cl)]$ (R = Pr^i **7a** *or* Me **7b**) *with* HCl.—Hydrogen chloride gas was passed through a suspension of $[N(PPh_3)_2][W_2(\eta\text{-}C_5H_4R)_2Cl_4(\mu\text{-}Cl)]$ **7** (*ca.* 0.25 mmol) in toluene (20 cm³) for 5 min at r.t. The initially colourless supernatant became red and an off-white solid ($[N(PPh_3)_2]Cl$) was observed. The solution was filtered, reduced in volume to *ca.* 5 cm³ and placed at −80 °C to afford $[W_2(\eta\text{-}C_5H_4R)_2Cl_4(\mu\text{-}Cl)(\mu\text{-}H)]$ (R = Pr^i **9a** or Me **9b**) which was characterised by comparison of its NMR spectrum with that of an authentic sample. Yield >90%.

Reaction of $[N(PPh_3)_2][Mo_2(\eta\text{-}C_5H_4Me)_2Cl_4(\mu\text{-}Cl)]$ **8** *with* HCl.—Hydrogen chloride gas was passed through a suspension of $[N(PPh_3)_2][Mo_2(\eta\text{-}C_5H_4Me)_2Cl_4(\mu\text{-}Cl)]$ **8** (300 mg, 0.28 mmol) in toluene (*ca.* 20 cm³) for 5 min at room temperature. The initially colourless supernatant turned brown and an off-white solid ($[N(PPh_3)_2]Cl$) was observed. The solution was filtered, reduced in volume to *ca.* 5 cm³ and placed at −80 °C to afford $[Mo_2(\eta\text{-}C_5H_4Me)_2(\mu\text{-}Cl)_4]$ which was characterised by comparison of its ¹H NMR spectrum with that of an authentic sample. Yield: >90%.

Preparation of $[W_2(\eta\text{-}C_5H_4R)_2Cl_3(\mu\text{-}Cl)(\mu\text{-}\sigma:\eta^2\text{-}R'CN)]$ (R′ = Me **10**, Et **11** *or* Ph **12**; R = Pr^i **a** *or* Me **b**).—A typical preparation is described. A suspension of $[W_2(\eta\text{-}C_5H_4R)_2Cl_4]$ (0.27 mmol) in light petroleum (*ca.* 20 cm³) was treated with an excess of R′CN (*ca.* 0.05 cm³) to give a brown solution. After 30 min the volatiles were removed and the residues washed with diethyl ether (2 × 10 cm³) and dried *in vacuo* to give $[W_2(\eta\text{-}C_5H_4R)_2Cl_3(\mu\text{-}Cl)(\mu\text{-}\sigma:\eta^2\text{-}R'CN)]$ as a red-brown or purple solid. Yield: 70–90%. For R′ = Et, R = Pr^i, the oily product always contained varying quantities of residual solvent. The compounds were not recrystallised due to their extreme moisture sensitivity which always resulted in contamination with hydrolysis products on further handling using Schlenk-line techniques.

Preparation of trans-$[W_2(\eta\text{-}C_5H_4R)_2Cl_4(\mu\text{-}Cl)(\mu\text{-}R'CNH)]$ (R′ = Me **13**, Et **14** *or* Ph **15**; R = Pr^i **a** *or* Me **b**).—A typical preparation is described. A suspension of $[W_2(\eta\text{-}C_5H_4R)_2Cl_4]$ (0.27 mmol) in diethyl ether (*ca.* 20 cm³) was treated with an excess of R′CN (*ca.* 0.05 cm³). The mixture was stirred for 30 min to give a red-brown or purple solution. Hydrogen chloride gas was bubbled through the solution for 3 min to afford an orange microcrystalline precipitate. The pale red supernatant was decanted and the residues washed with light petroleum (2 × 10 cm³) and dried *in vacuo* to afford orange microcrystals of *trans*-$[W_2(\eta\text{-}C_5H_4R)_2Cl_4(\mu\text{-}Cl)(\mu\text{-}R'CNH)]$. Yield: 85–90%.

Preparation of trans-$[W_2(\eta\text{-}C_5H_4Pr^i)_2Cl_4(\mu\text{-}Cl)(\mu\text{-}EtCND)]$ **14a-d**.—This compound was prepared from a brown diethyl ether solution of $[W_2(\eta\text{-}C_5H_4Pr^i)_2Cl_3(\mu\text{-}Cl)(\mu\text{-}\sigma:\eta^2\text{-}EtCN)]$ **11a** (prepared *in situ*) and DCl in a manner analogous to that described for the isotopomer **14a**.

Preparation of cis-$[W_2(\eta\text{-}C_5H_4R)_2Cl_4(\mu\text{-}Cl)(\mu\text{-}R'CNH)]$ (R′ = Me **16**, Et **17** *or* Ph **18**; R = Pr^i **a** *or* Me **b**.—Typical preparations are described.

Method (*i*). The orange complex *trans*-$[W_2(\eta\text{-}C_5H_4R)_2Cl_4$-

(μ-Cl)(μ-R′CNH)] (R′ = Me **13**, Et **14** or Ph **15**; R = Pr^i **a** or Me **b**) was dissolved in CH_2Cl_2 to give a red-purple solution after 30 min. Volatiles were removed under reduced pressure and the residues washed with light petroleum (2 × 10 cm^3) and dried *in vacuo* to afford the analytically pure, corresponding isomer *cis*-[W_2(η-C_5H_4R)$_2Cl_4$(μ-Cl)(μ-R′CNH)] as a red-purple solid in quantitative yield.

Method (*ii*) (R = Pr^i *only*). A solution of [W_2(η-$C_5H_4Pr^i$)$_2$-Cl_4] in toluene was treated with an excess of R′CN to give a brown solution. A drop of water was added to give a red-purple precipitate after 12 h. The supernatant was decanted and the residues washed with light petroleum (2 × 10 cm^3) and dried *in vacuo* to afford red-purple *cis*-[W_2(η-$C_5H_4Pr^i$)$_2Cl_4$(μ-Cl)(μ-R′CNH)]. Yield: 40–50%.

Preparation of cis-[W_2(η-$C_5H_4Pr^i$)$_2Cl_4$(μ-Cl)(μ-MeCND)] **16a–d**.—This compound was prepared from a toluene solution of [W_2(η-$C_5H_4Pr^i$)$_2Cl_3$(μ-Cl)(μ-σ:η^2-MeCN)] **10a** (prepared *in situ*) and [$^2H_2$]water in a manner analogous to that described for the isotopomer **16a** [method (*ii*) above].

X-Ray Crystal Structure Determinations of Complexes **4b**, **5** *and* **11b**.—Crystal data and data collection and processing parameters are given in Table 8. The general procedure was as follows. A crystal was sealed in a Lindemann glass capillary and transferred to the goniometer head of an Enraf-Nonius CAD4 diffractometer interfaced to a PDP 11/23 minicomputer. Unit-cell parameters were calculated from the setting angles of 25 carefully centred reflections. Three reflections were chosen as intensity standards and were measured every 3600 s of X-ray exposure time, and three orientation controls were measured every 250 reflections. The data were measured using graphite-monochromated Mo-Kα radiation (λ = 0.710 69 Å) and an ω–2θ scan mode. The crystal of complex **11b** was slightly split but the peak-to-peak separation was not more than 0.5° in ω.

The data were corrected for Lorentz and polarisation effects and an empirical absorption correction[28] based on an azimuthal scan was applied. Equivalent reflections were merged and systematically absent reflections rejected. The tungsten atom position(s) was determined from a Patterson synthesis. Subsequent Fourier difference syntheses revealed the positions of other non-hydrogen atoms. Non-hydrogen atoms were refined with anisotropic thermal parameters by full-matrix least-squares procedures and hydrogen atoms were placed in estimated positions (C–H 0.96) with fixed isotropic thermal parameters. For compound **11b** N(1) could not be successfully refined, possibly due to absorption problems. A Chebyshev weighting scheme[29] was applied and the data were corrected for the effects of anomalous dispersion and isotropic extinction (*via* an overall isotropic extinction parameter[30]) in the final stages of refinement. All crystallographic calculations were performed using the CRYSTALS suite[31] on a MicroVAX 3800 computer in the Chemical Crystallography Laboratory, Oxford. Neutral atom scattering factors were taken from the usual sources.[32]

Additional material available from the Cambridge Crystallographic Data Centre comprises H-atom coordinates, thermal parameters, and remaining bond lengths and angles.

Acknowledgements

We thank the Chinese government and CIRIT Generalitat de Catalunya for support (to Q. F. and M. F. respectively).

References

1 See, for example, (*a*) F. A. Cotton and R. A. Walton, *Multiple Bonds Between Metal Atoms*, Wiley, New York, 1982; *Struct. Bonding* (*Berlin*), 1985, **62**, 1; (*b*) M. J. Winter, *Adv. Organomet. Chem.*, 1989, **29**, 101; W. A. Buhro and M. H. Chisholm, *Adv. Organomet. Chem.*, 1987, **27**, 311.

2 M. L. H. Green, J. D. Hubert and P. Mountford, *J. Chem. Soc., Dalton Trans.*, 1990, 3793.

3 Q. Feng, M. Ferrer, M. L. H. Green, P. C. McGowan, P. Mountford and V. S. B. Mtetwa, *J. Chem. Soc., Chem. Commun.*, 1991, 552.

4 M. L. H. Green and P. Mountford, *J. Chem. Soc., Chem. Commun.*, 1989, 732.

5 R. D. Adams, D. M. Collins and F. A. Cotton, *Inorg. Chem.*, 1974, **13**, 1086.

6 D. S. P. Rogers, D.Phil. Thesis, Oxford, 1984.

7 C. Couldwell and C. K. Prout, *Acta Crystallogr., Sect. B*, 1978, **34**, 933.

8 W. A. Herrmann, R. A. Fischer and E. Herdtweck, *J. Organomet. Chem.*, 1987, **239**, C1.

9 M. D. Curtis and J. Real, *Organometallics*, 1985, **4**, 940.

10 R. F. Bryan, P. T. Greene, M. J. Newlands and D. S. Field, *J. Chem. Soc. A*, 1970, 3068.

11 B. E. Bursten and R. H. Cayton, *Inorg. Chem.*, 1989, **28**, 2846; E. D. Jemmis, A. R. Pinhas and R. Hoffmann, *J. Am. Chem. Soc.*, 1980, **102**, 2576.

12 P. D. Grebenik, M. L. H. Green, A. Izquierdo, V. S. B. Mtetwa and C. K. Prout, *J. Chem. Soc., Dalton Trans.*, 1987, 9.

13 M. L. H. Green and W. E. Lindsell, *J. Chem. Soc. A*, 1967, 686.

14 L. Pauling, *The Nature of the Chemical Bond*, 3rd edn., Cornell University Press, 1960; A. G. Orpen, L. Brammer, F. H. Allen, O. Kennard, D. G. Watson and R. Taylor, *J. Chem. Soc., Dalton Trans.*, 1989, S1.

15 E. Singleton and H. E. Oosthuizen, *Adv. Orgomet. Chem.*, 1983, **23**, 209.

16 M. Green, J. A. K. Howard, M. Murray, J. L. Spencer and F. G. A. Stone, *J. Chem. Soc., Dalton Trans.*, 1977, 1509.

17 M. Novotny, D. F. Lewis and S. J. Lippard, *J. Am. Chem. Soc.*, 1972, **94**, 6961.

18 I. Ugi, R. Meyer, M. Lipinski, F. Bodesheim and F. Rosendahl, *Org. Synth.*, 1961, **41**, 13.

19 R. D. Adams, D. A. Katahira and L. W. Yang, *Organometallics*, 1982, **1**, 231; F. A. Cotton and B. A. Frenz, *Inorg. Chem.*, 1974, **13**, 253; R. D. Adams, F. A. Cotton and G. A. Rusholme, *J. Coord. Chem.*, 1971, **1**, 275; L. S. Benner, M. M. Olmstead and M. M. Balch, *J. Organomet. Chem.*, 1978, **159**, 289.

20 R. Poli and A. L. Rheingold, *J. Chem. Soc., Chem. Commun.*, 1990, 552.

21 J. Sandström, *Dynamic N.M.R. Spectroscopy*, Academic Press, London, 1982.

22 Q. Feng, M. Ferrer, M. L. H. Green, P. Mountford, V. S. B. Mtetwa and K. Prout, *J. Chem. Soc., Dalton Trans.*, 1991, 1397.

23 F. A. Cotton and G. Wilkinson, *Advanced Inorganic Chemistry*, 5th edn., Interscience, New York, 1988.

24 M. H. Chisholm, F. A. Cotton, M. W. Extine and L. A. Rankel, *J. Am. Chem. Soc.*, 1978, **100**, 807; M. H. Chisholm, J. C. Huffman and N. S. Marchant, *J. Am. Chem. Soc.*, 1983, **105**, 6162; M. H. Chisholm, K. Folting, J. C. Huffman and N. S. Marchant, *Polyhedron*, 1984, **3**, 1033.

25 R. D. Adams and D. F. Chodosh, *Inorg. Chem.*, 1978, **17**, 41; W. R. Roper, G. E. Taylor, J. M. Waters and L. J. Wright, *J. Organomet. Chem.*, 1978, **157**, C27; F. Van Bolhnis, E. J. M. deBoer and J. H. Teuben, *J. Organomet. Chem.*, 1979, **170**, 299; A. K. McMullen, I. P. Rothwell and J. C. Huffman, *J. Am. Chem. Soc.*, 1985, **107**, 1072; F. H. Elsner, T. D. Tilley, A. L. Rheingold and S. J. Geib, *J. Organomet. Chem.*, 1988, **358**, 169; A. C. Sullivan, G. Wilkinson, M. Motevalli and M. B. Hursthouse, *J. Chem. Soc., Dalton Trans.*, 1988, 53; M. Bochmann, L. M. Wilson, M. B. Hursthouse and R. L. Short, *Organometallics*, 1987, **6**, 2556.

26 D. M. Hoffman, R. Hoffmann and C. R. Fisel, *J. Am. Chem. Soc.*, 1982, **104**, 3858.

27 For example, see refs. 1(*b*) and 26; R. S. Dickson and P. J. Fraser, *Adv. Organomet. Chem.*, 1974, **12**, 323; J. C. T. R. Burkett-St. Laurent, P. B. Hitchcock, H. W. Kroto, M. F. Meidine and J. F. Nixon, *J. Organomet. Chem.*, 1981, **238**, C82; R. Bartsch, P. B. Hitchcock, M. F. Meidine and J. F. Nixon *J. Organomet. Chem.*, 1984, **266**, C41; K. Sünkel, K. Schloter, W. Beck, K. Ackermann and H. Schubert, *J. Organomet. Chem.*, 1983, **241**, 333; M. R. Churchill and H. J. Wasserman, *Inorg. Chem.*, 1982, **21**, 226; H. Alper, F. W. B. Einstein, F. W. Harstock and A. C. Willis, *J. Am. Chem. Soc.*, 1985, **107**, 173.

28 A. C. T. North, D. C. Philips, and F. S. Mathews, *Acta Crystallogr., Sect. A*, 1968, **24**, 351.

29 J. S. Rollet, *Computing Methods in Crystallography*, Pergamon, Oxford, 1965.

30 A. C. Larson, *Acta Crystallogr., Sect. A*, 1967, **23**, 664.

31 D. J. Watkin, J. R. Carruthers and P. W. Betteridge, *CRYSTALS User Guide*, Chemical Crystallography Laboratory, University of Oxford, 1985.

32 *International Tables for X-Ray Crystallography*, Kynoch Press, Birmingham, 1974, vol. 4.

Received 14*th October* 1991; *Paper* 1/05205E